U. of Richmond
Radio Synchrotron Background Conference

July 21, 2017

Synchrotron Radiation as a Foreground to the Global Redshifted 21-cm Measurement by EDGES

Raul A. Monsalve

University of Colorado Boulder - Arizona State University

Take Home Message:

1) EDGES is ruling out an important set of physical models for the Global 21-cm Signal, and has sensitivity that would allow detection.

2) Current focus is on understanding the measurements at the mK level.

3) Accuracy of the diffuse galactic and extragalactic foreground model is of great importance for this purpose.

The Global Redshifted 21-cm Signal

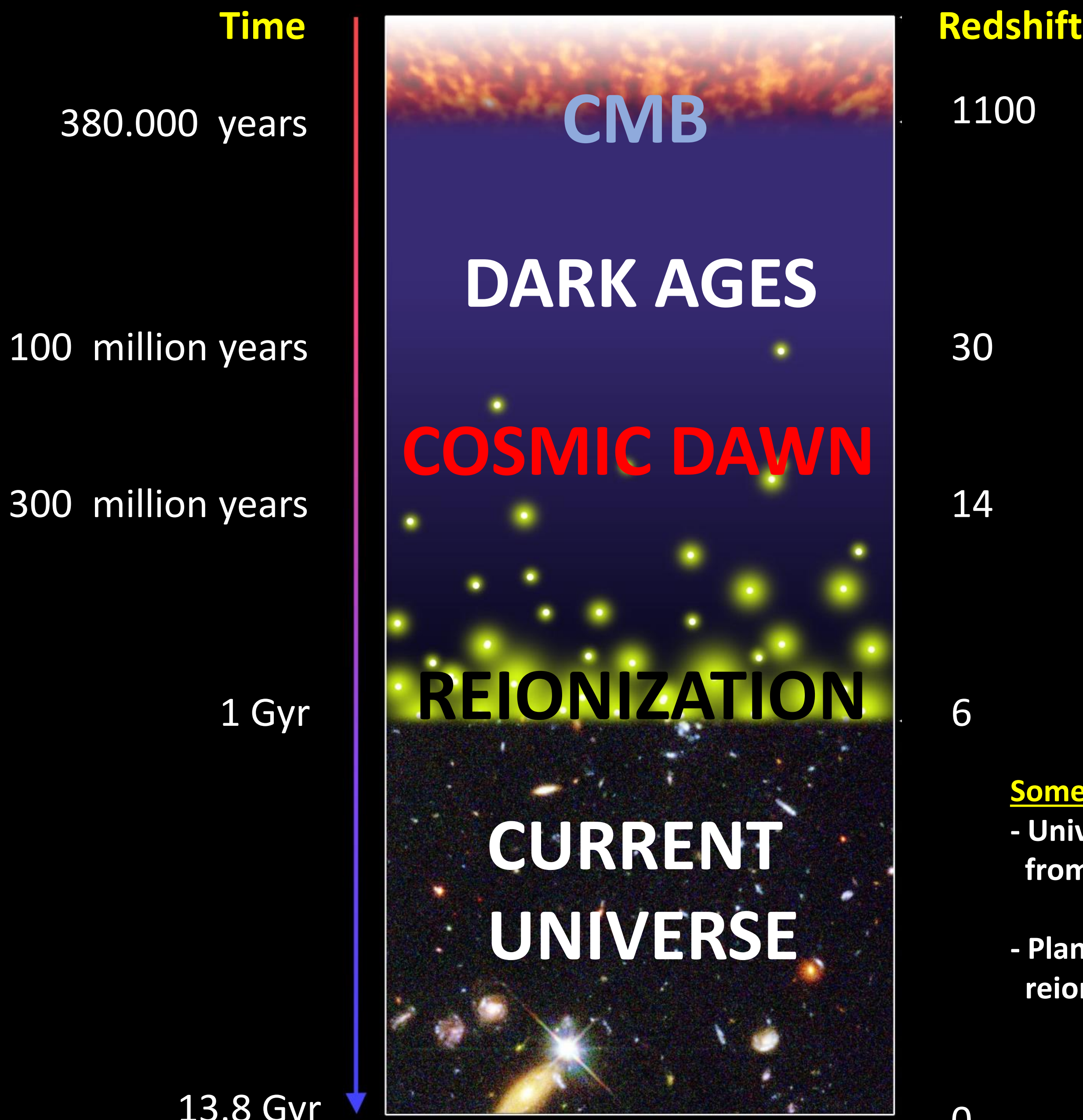

S.G. Djorgovski et al. & Digital Media Center, Caltech

Some Constraints on Reionization:

- Universe ionized by $z \sim 6$ from Gunn-Peterson trough (Fan et al. 2002).

- Planck collaboration et al. (2016) suggest reionization redshift of $z_r = 8.5 \pm 1$.

Emission at 21-cm from Hydrogen Atom

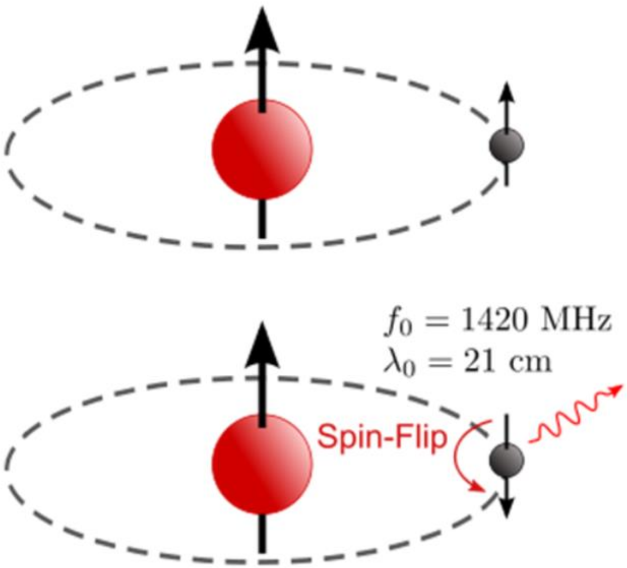

Parallel spins
Upper ground state

Anti-parallel spins
Lower ground state

Due to Cosmological Expansion

Redshift	Frequency
0	1420 MHz
6	200 MHz
35	40 MHz

$$\upsilon_{\text{obs}} = \frac{\upsilon_{\text{emit}}}{(1+z)}$$

21-cm Cosmology

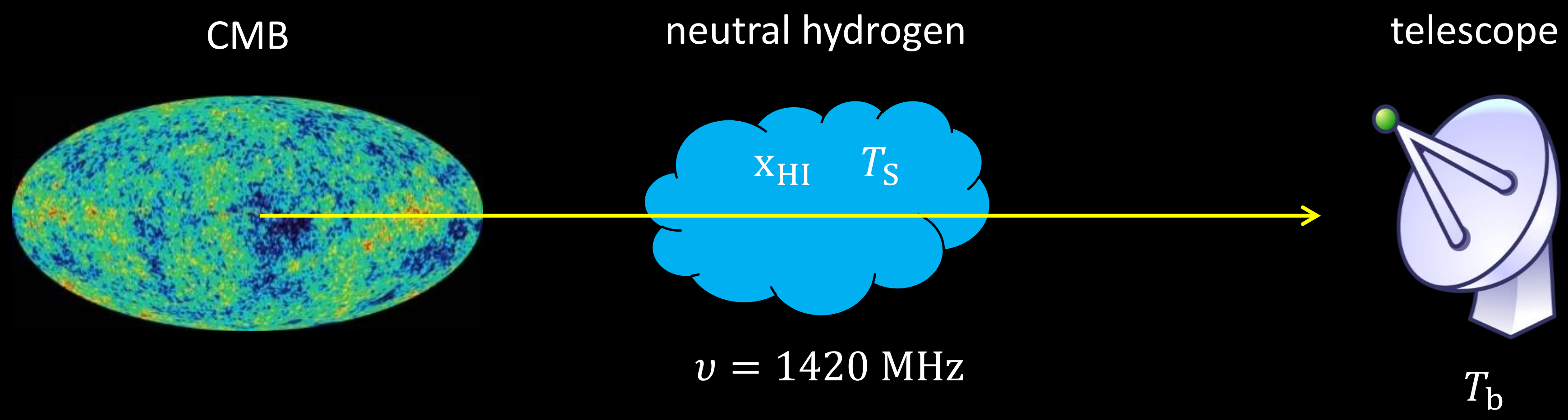

Cosmological Brightness Temperature

$$T_{21}(\theta, z) \approx 28\,\mathrm{mK} \cdot (1+\delta) \cdot \sqrt{\frac{1+z}{10}} \cdot x_{HI} \cdot \left(\frac{T_S - T_{CMB}}{T_S}\right)$$

fraction of neutral hydrogen (x_{HI})

spin temperature (T_S)

Spin Temperature

$$\frac{n_{\mathrm{upper}}}{n_{\mathrm{lower}}} = 3 \cdot exp\left(-\frac{h \cdot \upsilon_{21\mathrm{cm}}}{k_{\mathrm{b}} \cdot \boldsymbol{T_S}}\right)$$

$\upsilon_{21\mathrm{cm}} = 1420\ \mathrm{MHz}$
h : Planck constant
k_{b} : Boltzmann constant

http://www.cv.nrao.edu/course/astr534/HILine.html

$$\boldsymbol{T_S}^{-1} \approx \frac{T_{\mathrm{CMB}}^{-1} + x_{\mathrm{c}} T_{\mathrm{K}}^{-1} + x_{\alpha} T_{\alpha}^{-1}}{1 + x_{\mathrm{c}} + x_{\alpha}}$$

T_{K}: kinetic temperature of the gas
T_{α}: color temperature of Lyα photons
x_{c}: coupling due to collisions
x_{α}: coupling due to Wouthuysen-Field effect

Global (sky-average) 21-cm Signal

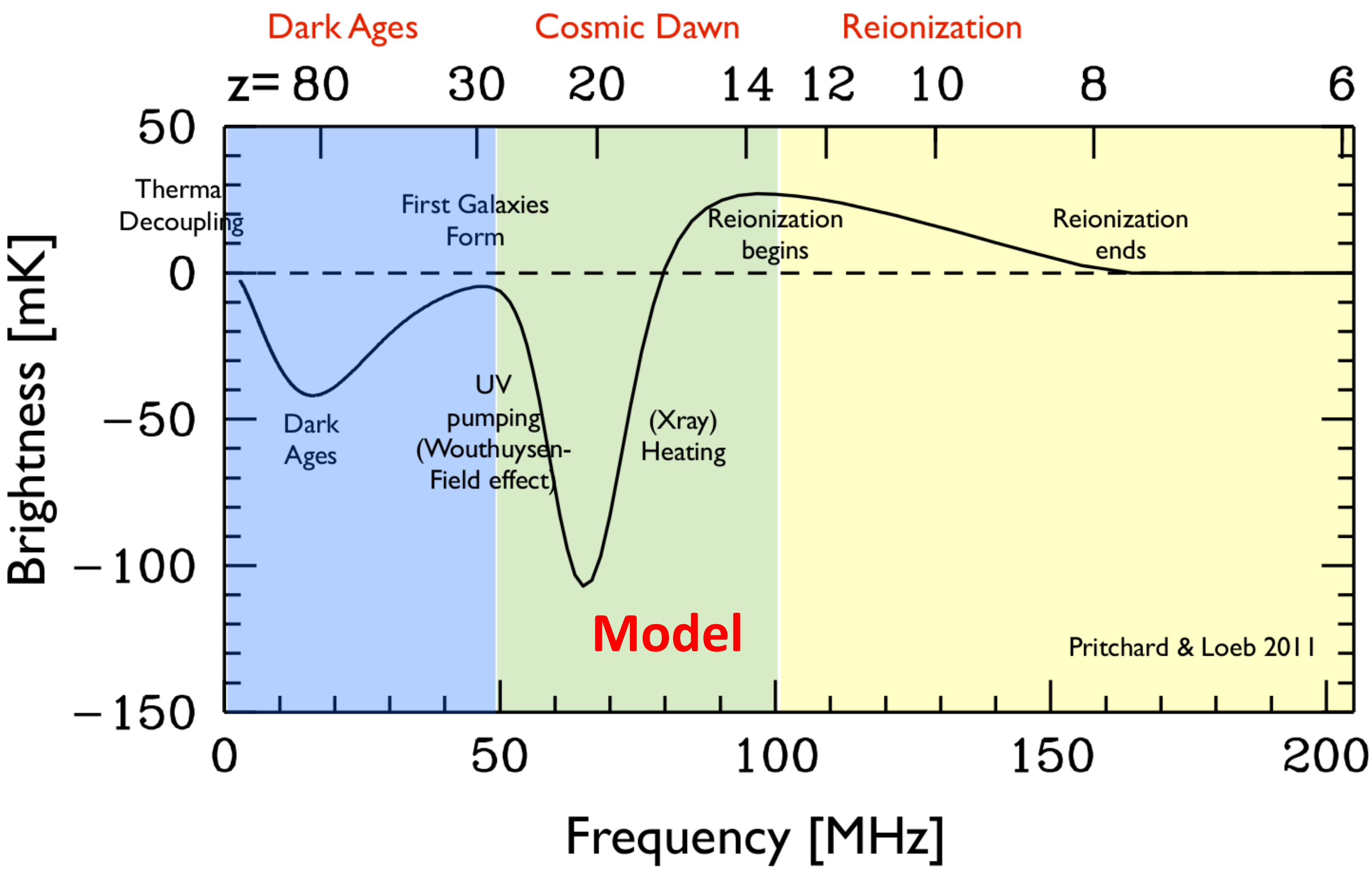

Global Signal for Different Scenarios

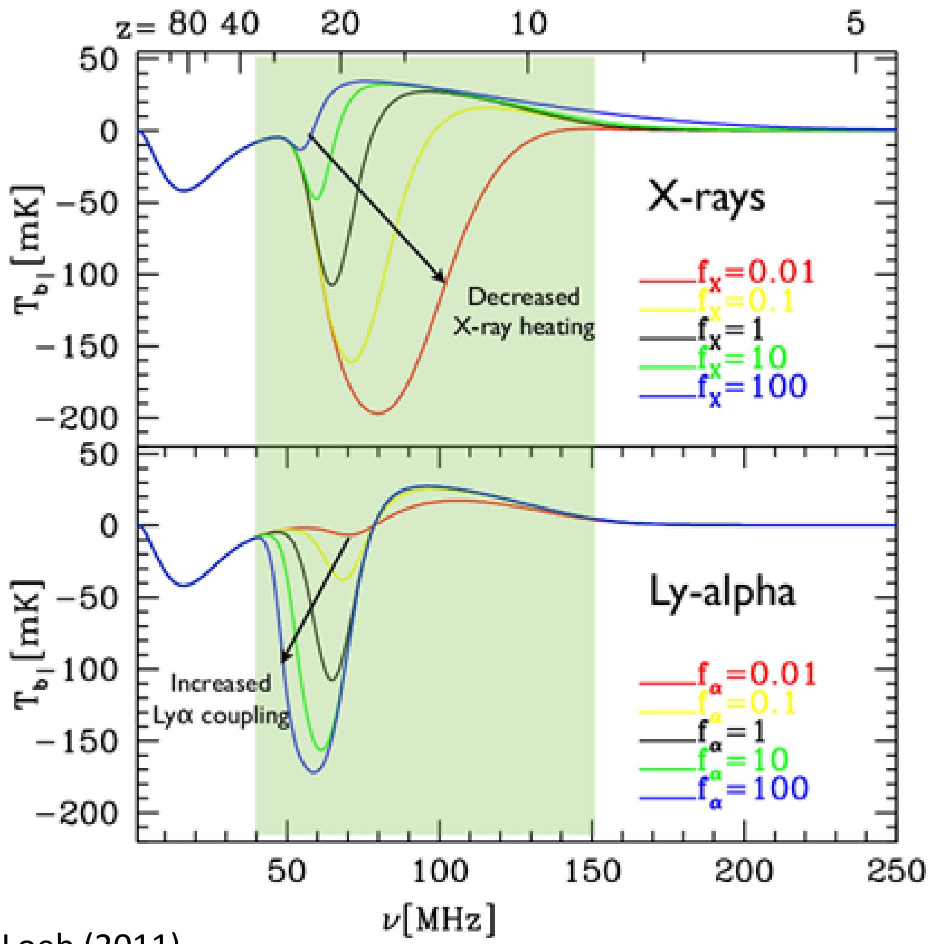

Pritchard & Loeb (2011)

Global Signal Examples

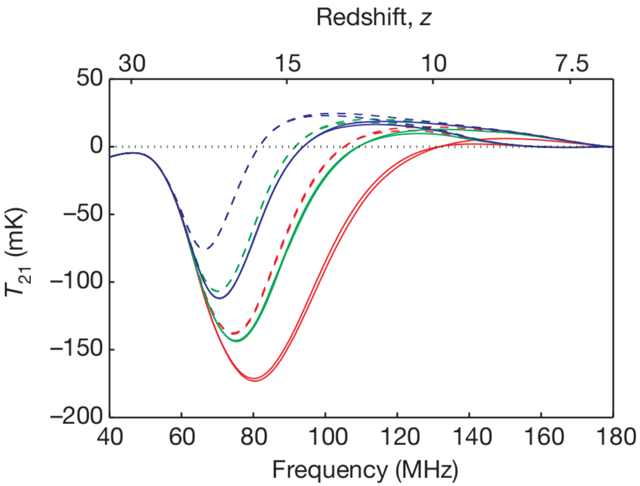

Fialkov et al. (2014)

- Semi-numerical.
- Hard spectra of X-ray binaries.

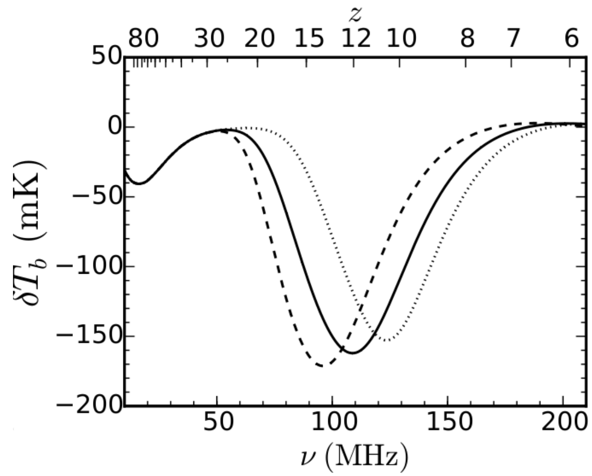

Mirocha et al. (2017)

- Analytical.
- No Pop III stars.
- $z < 8$ galaxy luminosity function extrapolated to lower luminosities and higher redshifts.
- Inefficient heating induced by XRBs with hard spectra.

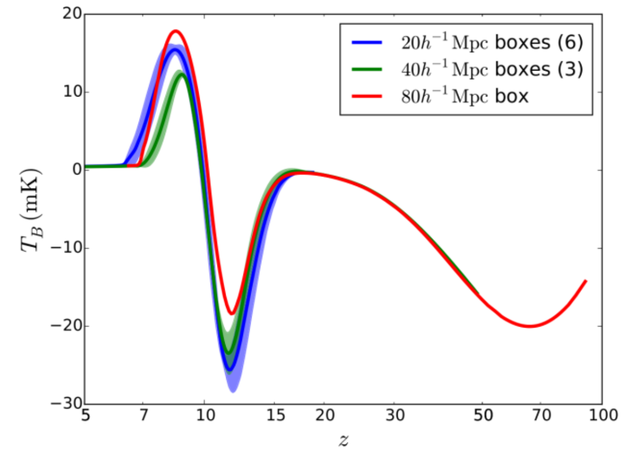

Kaurov & Gnedin (2016)

Uncertainty in models is high.

Analogy with the CMB

CMB

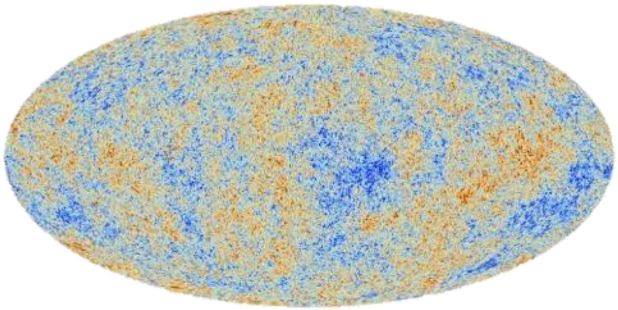

21-cm

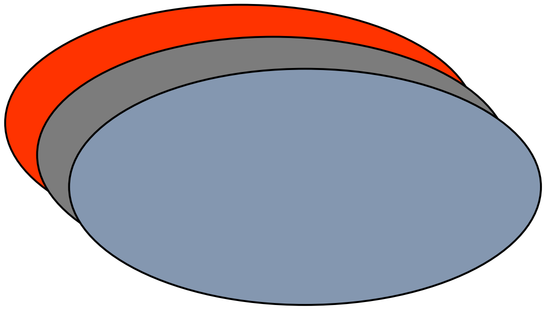

Measurements vs. frequency

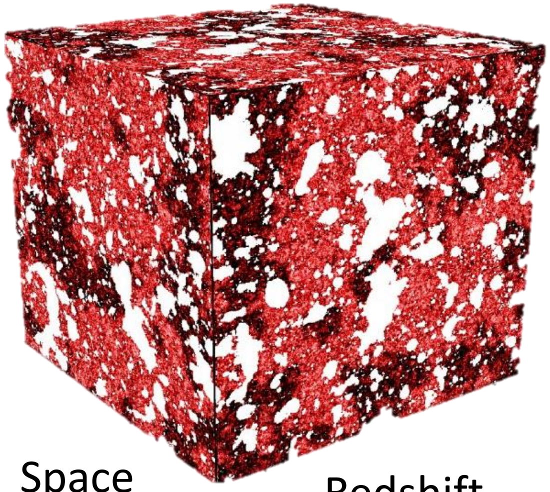

Arrays Targeting the EoR (> 100 MHz)

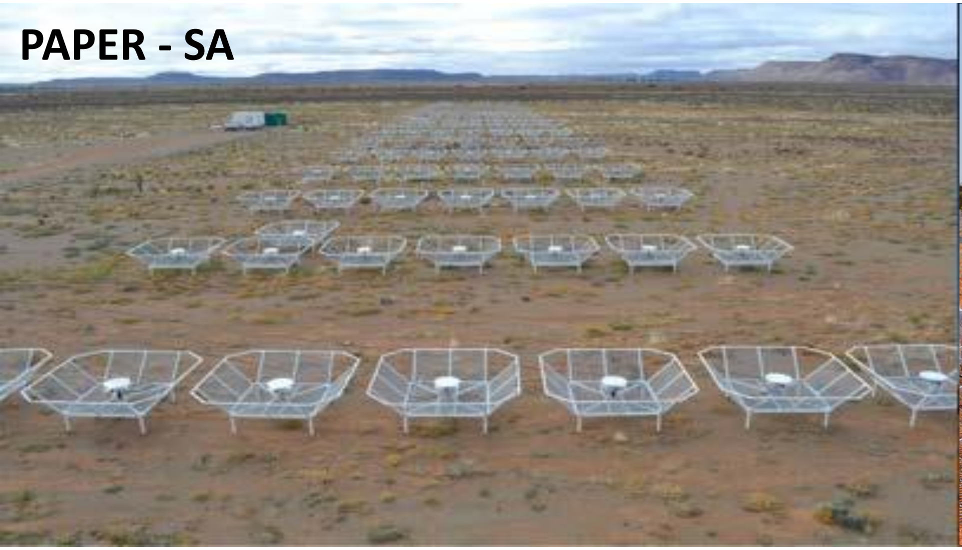

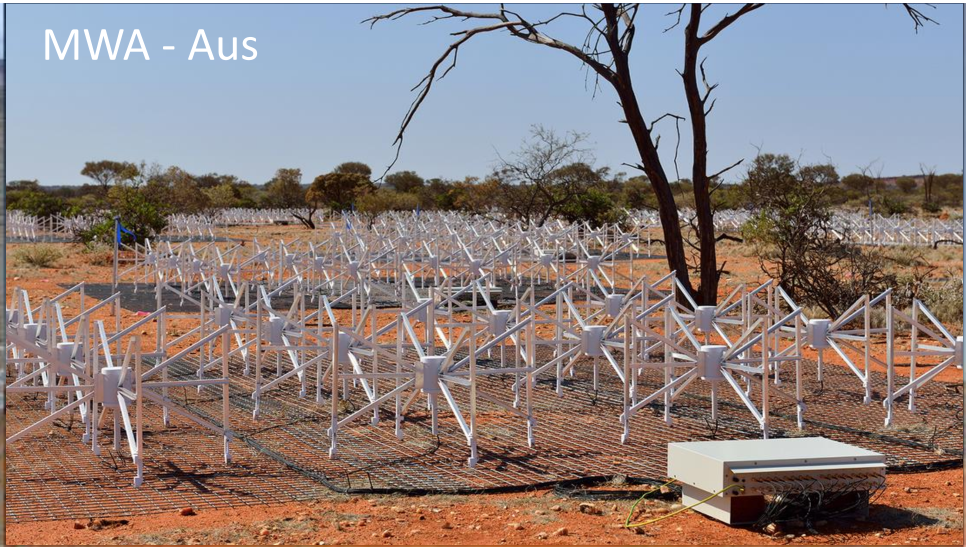

Array	FoV deg^2	Area m^2	Type	$FWHM_{150}$ arcmin	PS S/N* FG Avoidance	PS S/N* FG Removal	Start date
PAPER-128	1600	1200	Dipole	23	1.2	4.8	2013
MWA-128 Im	300	3600	Tile	10	0.6	6.4	2013
LOFAR Im	25	36000	Tile	5	1.4	17	2013
HERA-331	64	54000	Dish	20	23	91	2018
SKA-I Low Im	30	420000	Tile	5	13	140	2021+

LWA New Mexico / OVRO: @ lower frequencies

Power Spectrum of Anisotropies

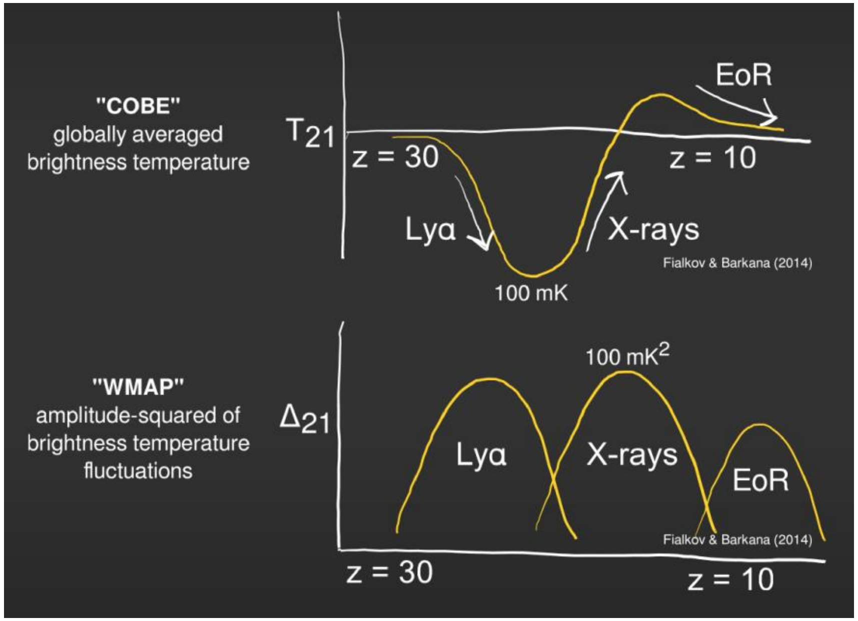

Credit:
M. Eastwood

Redshift Evolution

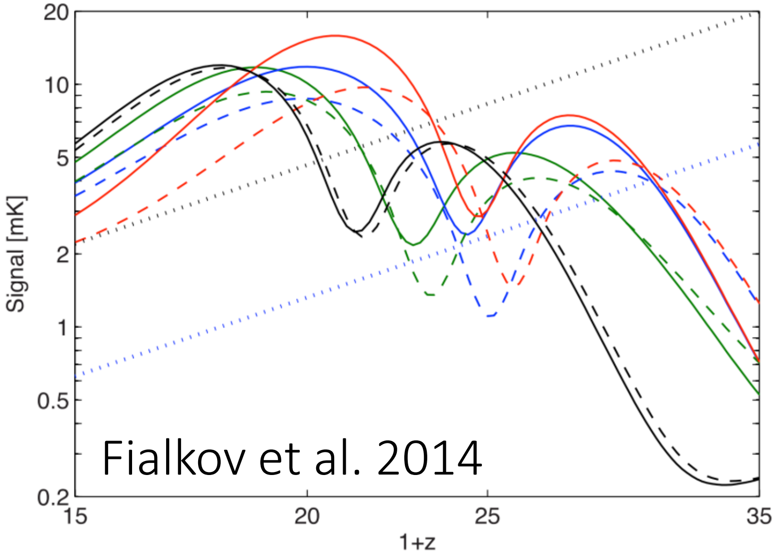

Scale Dependence

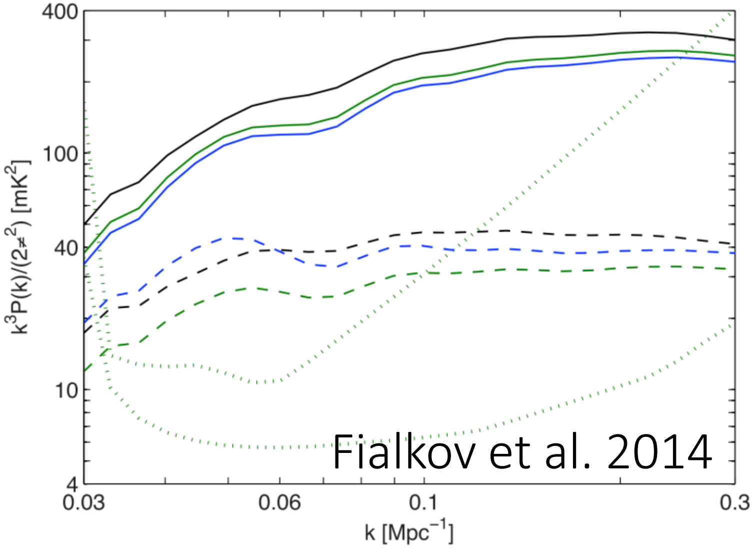

Real Progress in Techniques and Science from Arrays

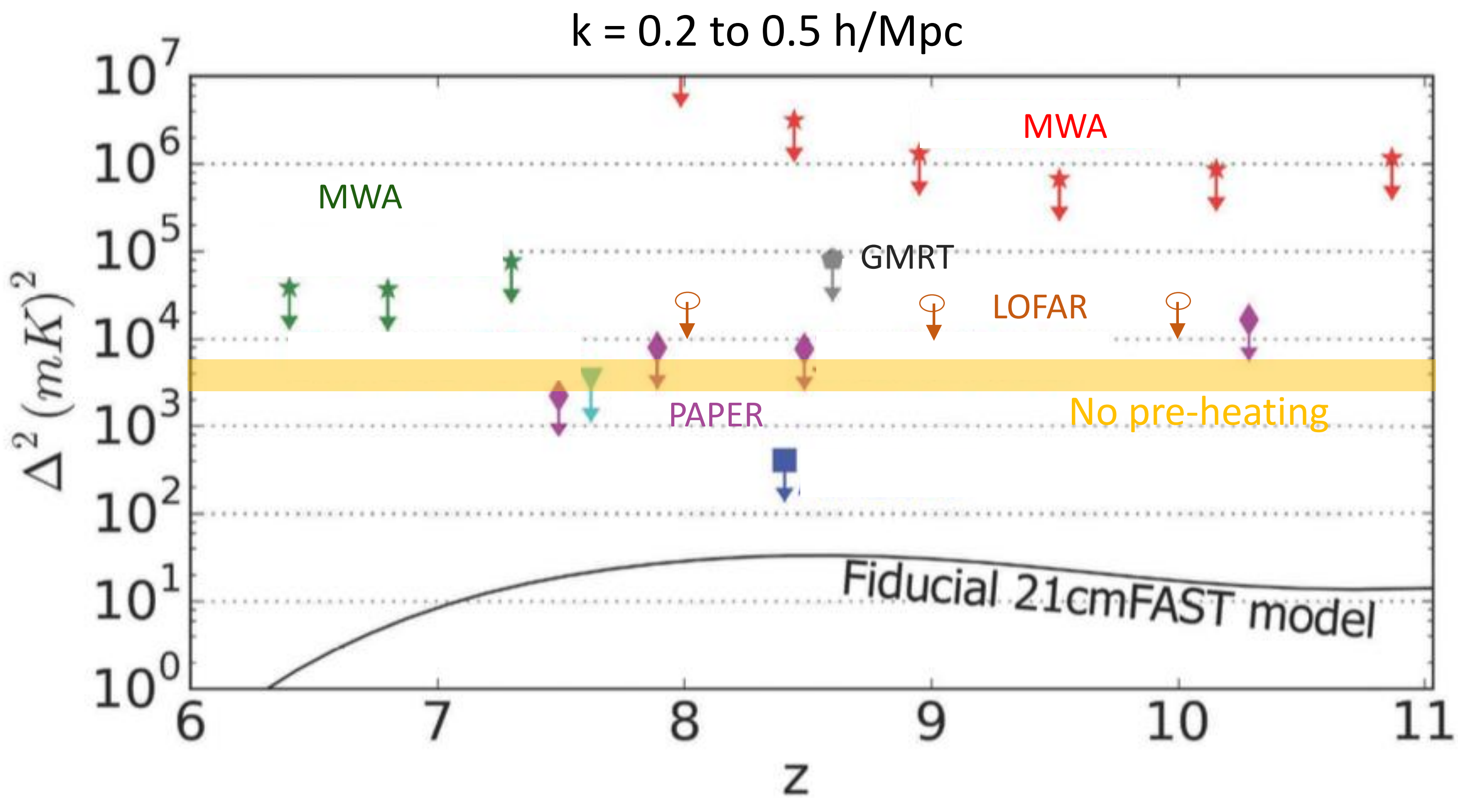

First astrophysically relevant limits from PAPER:
Early pre-heating of neutral IGM before reionization

Why Global Measurements

1) Direct probe of the average **gas temperature (kinetic and spin)** and **fraction** of neutral hydrogen.
2) This provides **constraints** on:
   - star and galaxy formation history
   - early feedback mechanisms
   - heating of the IGM
   - redshift and duration of epoch of reionization
3) "**Simpler" instrumentation** than arrays.
4) One of the few current **alternatives** to probe Cosmic Dawn ($z > 14$) period.

Challenges

1) **Hard instrument calibration** problem.
2) **Strong diffuse foregrounds** compared to signal.

Observational Status

No Cosmological 21-cm Signal Detected Yet

Constraints on the global signal from EDGES, LEDA, SCIHI, SARAS

Diffuse Foregrounds

Foreground Temperature

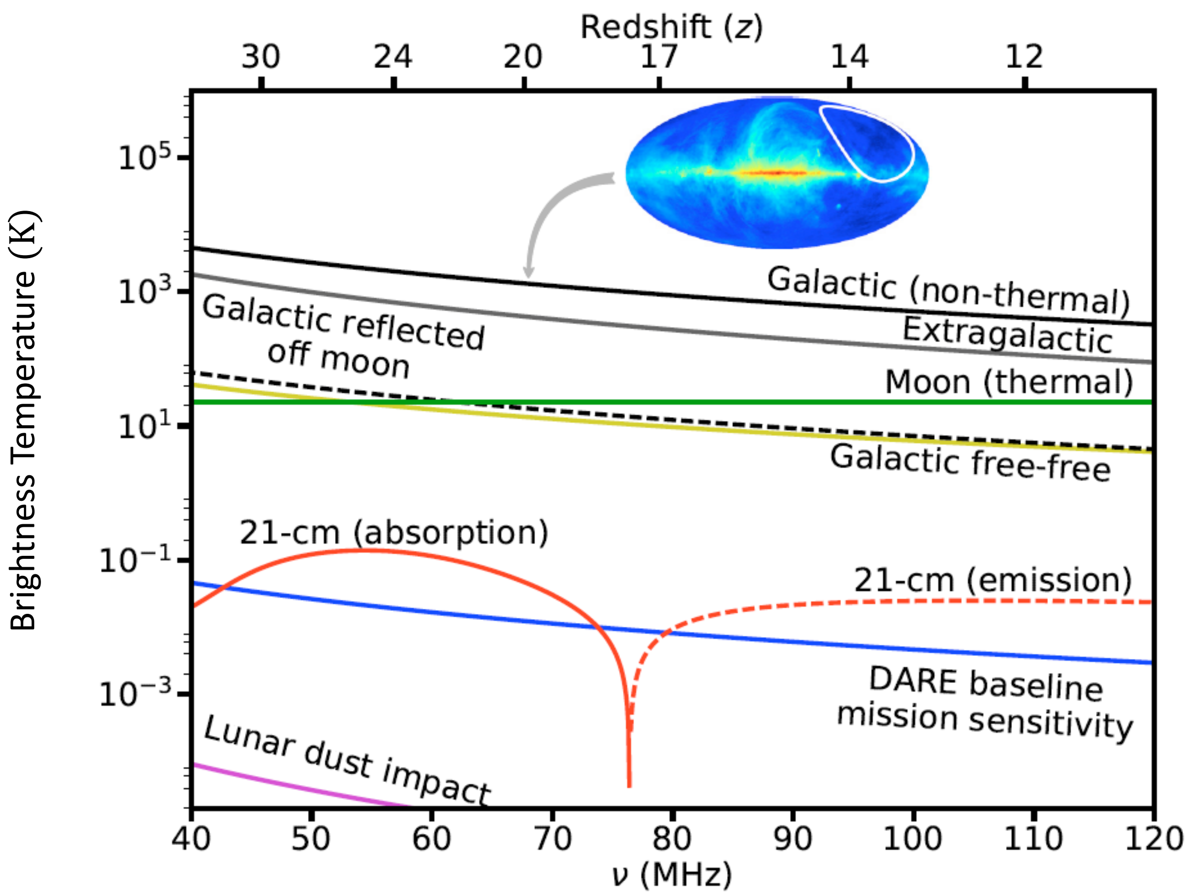

Dark Ages Radio Explorer (DARE)
Proposed to NASA MIDEX program in Dec 2016

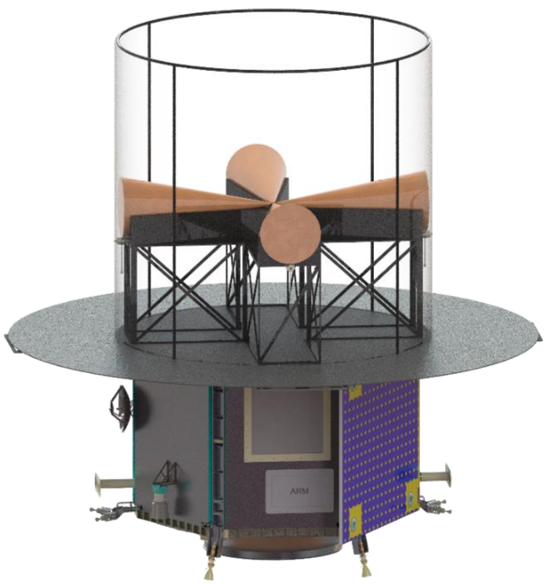

45-MHz Map

Guzmán et al. (2011)

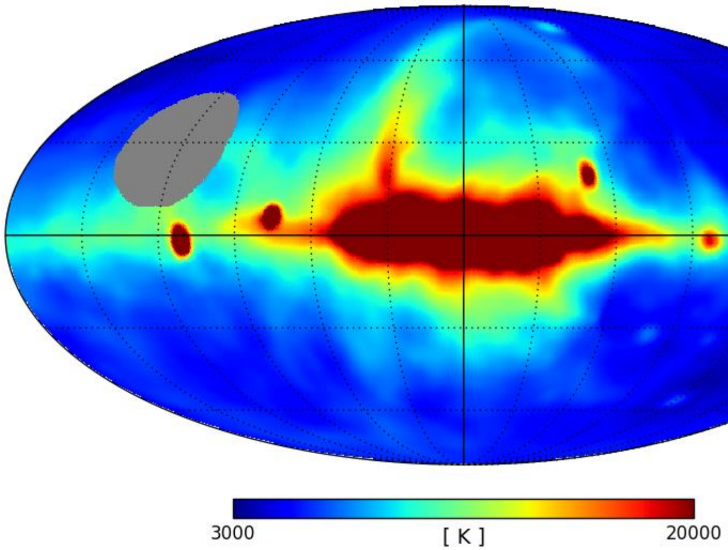

408-MHz Map

Haslam et al. (1982)

Remazeilles et al. (2014)

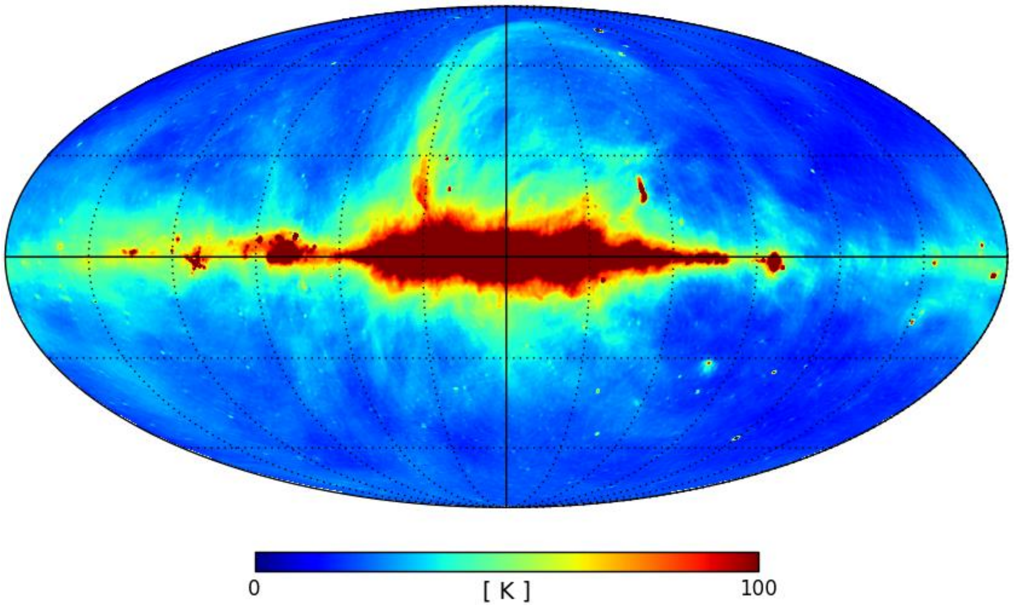

1) Used for **calibration and simulation of observations**.
2) From **hundreds to thousands of Kelvins**.
3) Include **Galactic and Extragalactic**.
4) Mostly **synchrotron radiation**.
5) Large **spatial gradients**.
6) Techniques suggested to **take advantage of these gradients** for signal separation (e.g. Liu et al. 2013, Switzer & Liu 2014).

Global Sky Models

Oliveira-Costa et al. (2008)

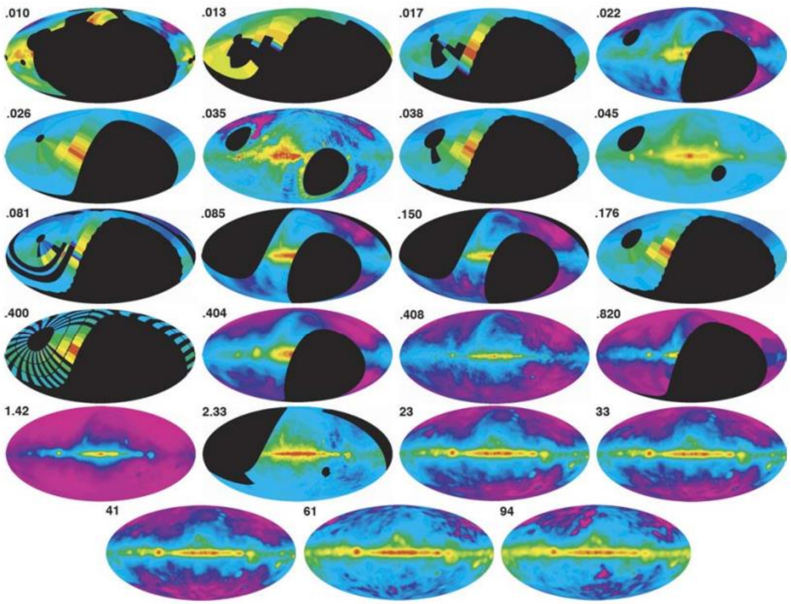

Zheng et al. (2017)

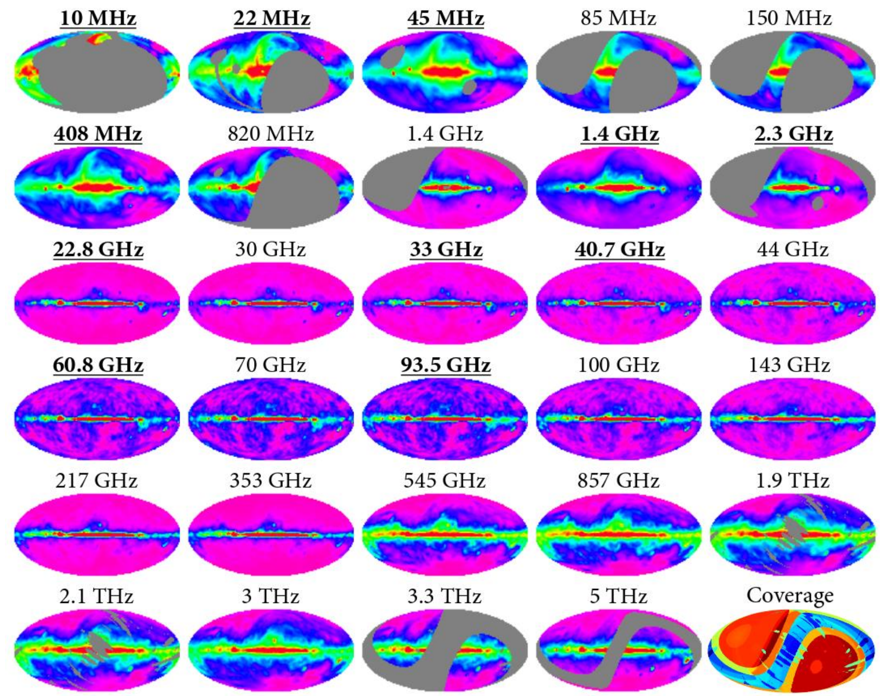

1) **Sky models** from MHz to THz.
2) **Interpolation** requires **up to 5 terms**.
3) **Spectral smoothness** supported by, i.e.:
   - **Theoretical models** (Bernardi et al. 2015)
   - **Measurements from ARCADE- 2** (Kogut et al. 2011; Kogut 2012)

Also:
Sathyanarayana Rao et al. (2016)

Polarized Diffuse Foreground

1) Cosmological signal is **NOT polarized**.
2) Diffuse foreground is **polarized** ($\leq 5\%$) (Lenc et al. 2016).
3) **Potential leakage** from Polarized signal to Unpolarized Intensity.
4) **Potential introduction of spectral structure** due to Faraday Rotation.
5) From simulations, **low impact expected** on the Global 21-cm signal due to beam dilution.

Observation with MWA ~150 MHz
Low-foreground region
Lenc et al. (2016)

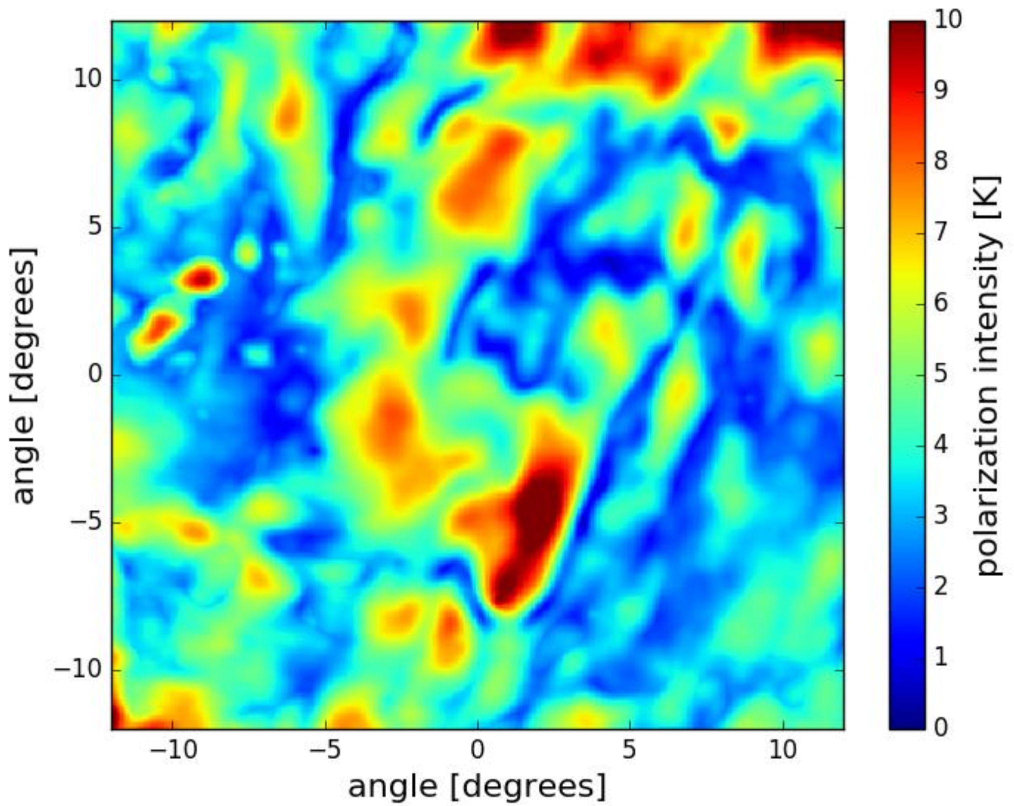

Induced Polarization Technique

1) Technique based on the **modulation of foregrounds**.
2) **Foreground** varies spatially but is **spectrally smooth**.
3) **Global 21-cm** signal is spatially uniform but **spectrally complex**.
4) Frequency-dependent modulation amplitude represents **the foreground alone, and is contained in Stokes Q**.
5) **Stokes I contains both**, foreground and 21-cm signal.
6) Tested on the ground, **in preparation for DARE**.

University of Colorado Boulder

National Radio Astronomy Observatory

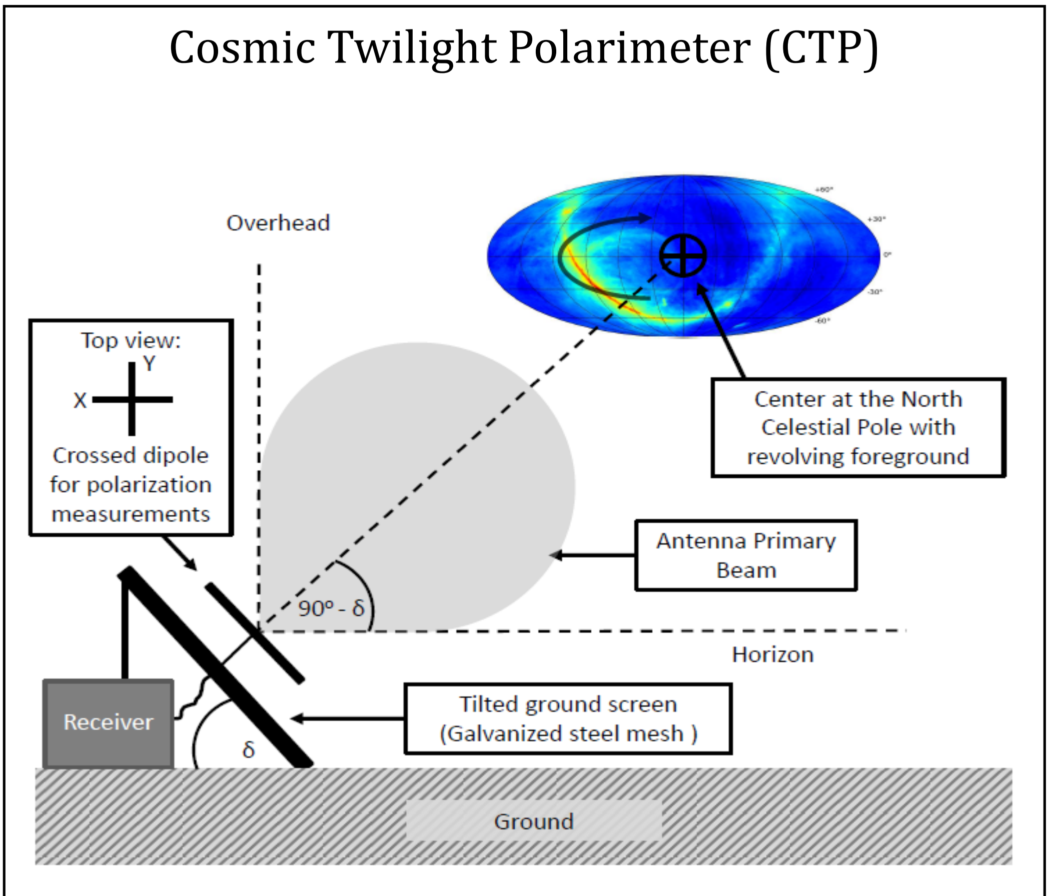

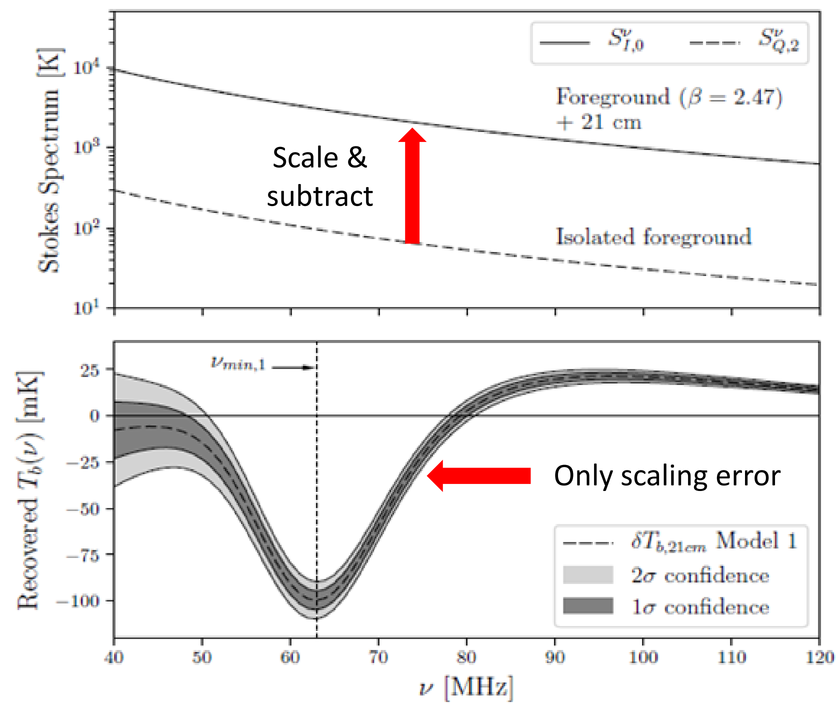

Nhan et al. (2017)

Global Experiments

BIGHORNS
(Curtin U., Australia, Sokolowsky et al.)

SARAS
(RRI, India, Subrahmanjan et al.)

HYPERION
(Berkeley)

SCI-HI -> PRIZM
(Carnegie Mellon, Peterson et al.)

LEDA
(Harvard, Caltech, Greenhill et al.)

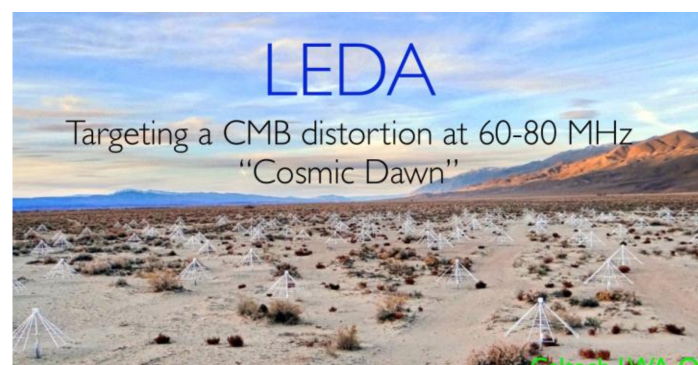

EDGES

Experiment to Detect the Global EoR Signature

Prof. Judd Bowman (PI)
Dr. Alan Rogers
Dr. Raul Monsalve
Mr. Thomas Mozdzen
Ms. Nivedita Mahesh

Arizona State University
University of Colorado Boulder
MIT Haystack Observatory

Location


EDGES
A
MRO
Western Australia
Northern Territory
Australia
Queensland
South Australia
New South Wales
Perth
Adelaide
Brisbane
Gold Coast
Sydney
Australian Capital Territory
Victoria
Melbourne
Great Australian Bight
Map data ©2014 GBRMPA, Google

Murchison Radio-astronomy Observatory (MRO)

Radio-Quiet Site

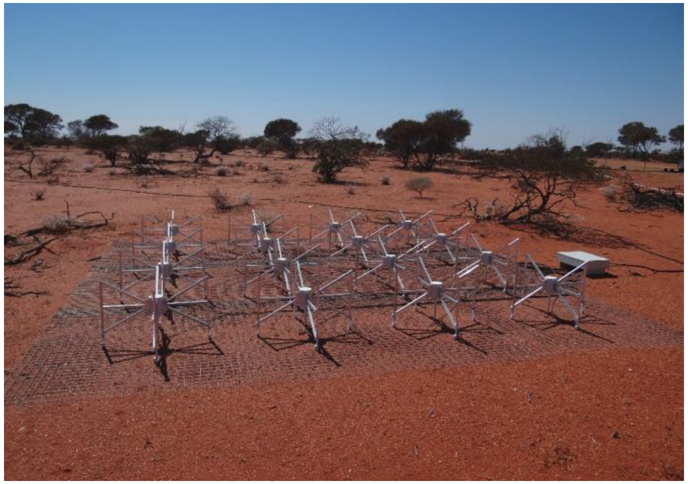

Two EDGES Instruments

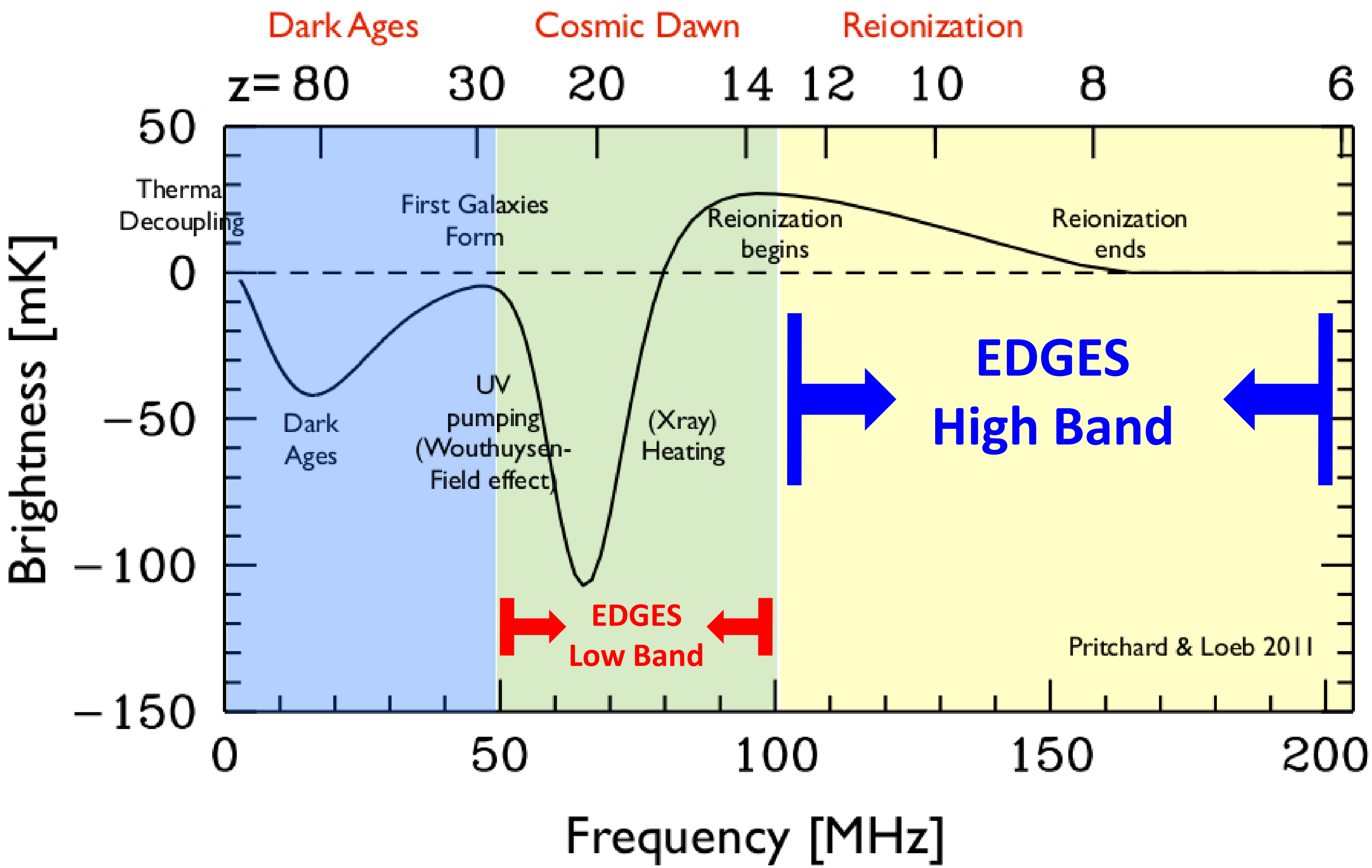

EDGES Block Diagram

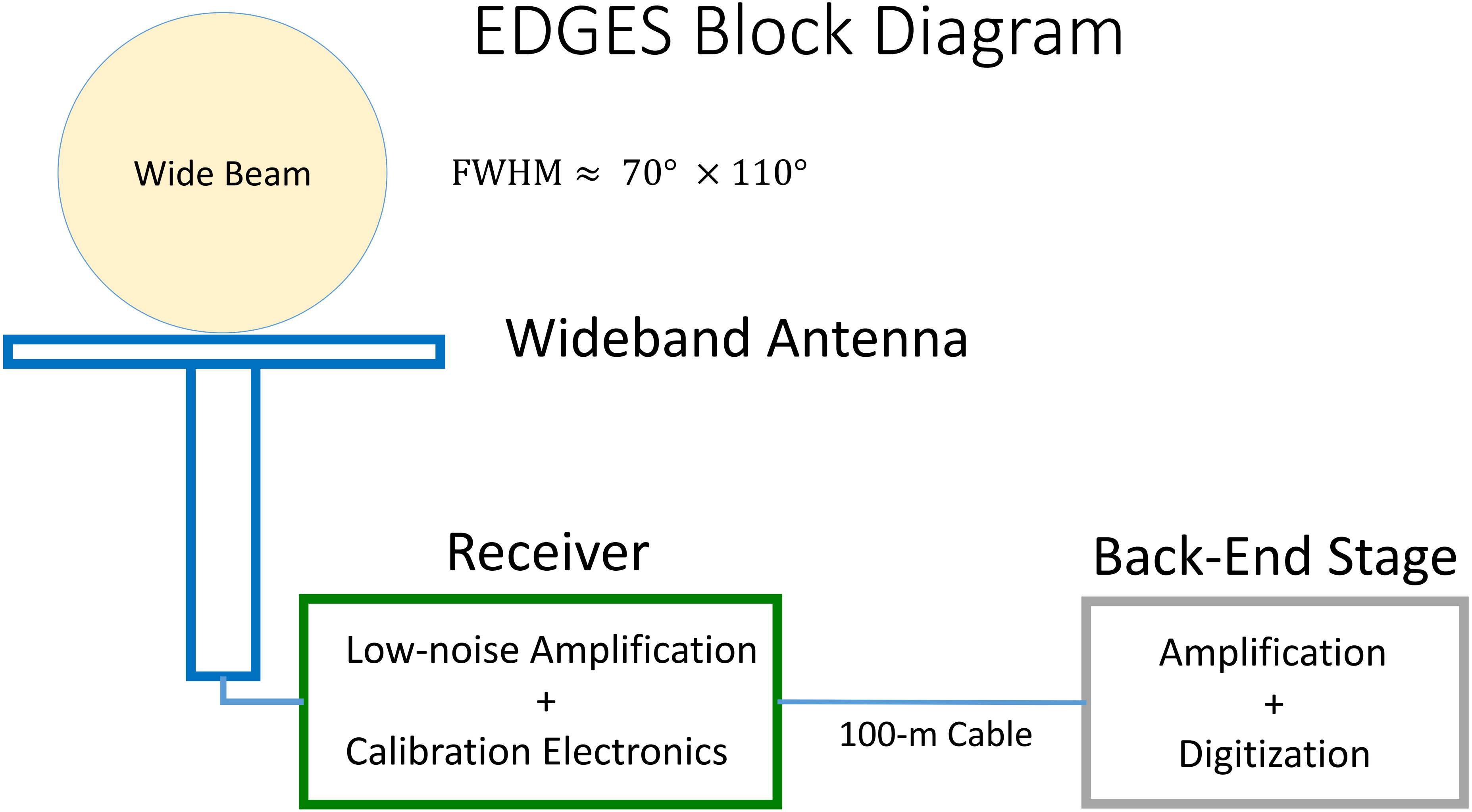

Details in:
Mozdzen et al. (2016)
Monsalve et al. (2017)

Current EDGES Instruments

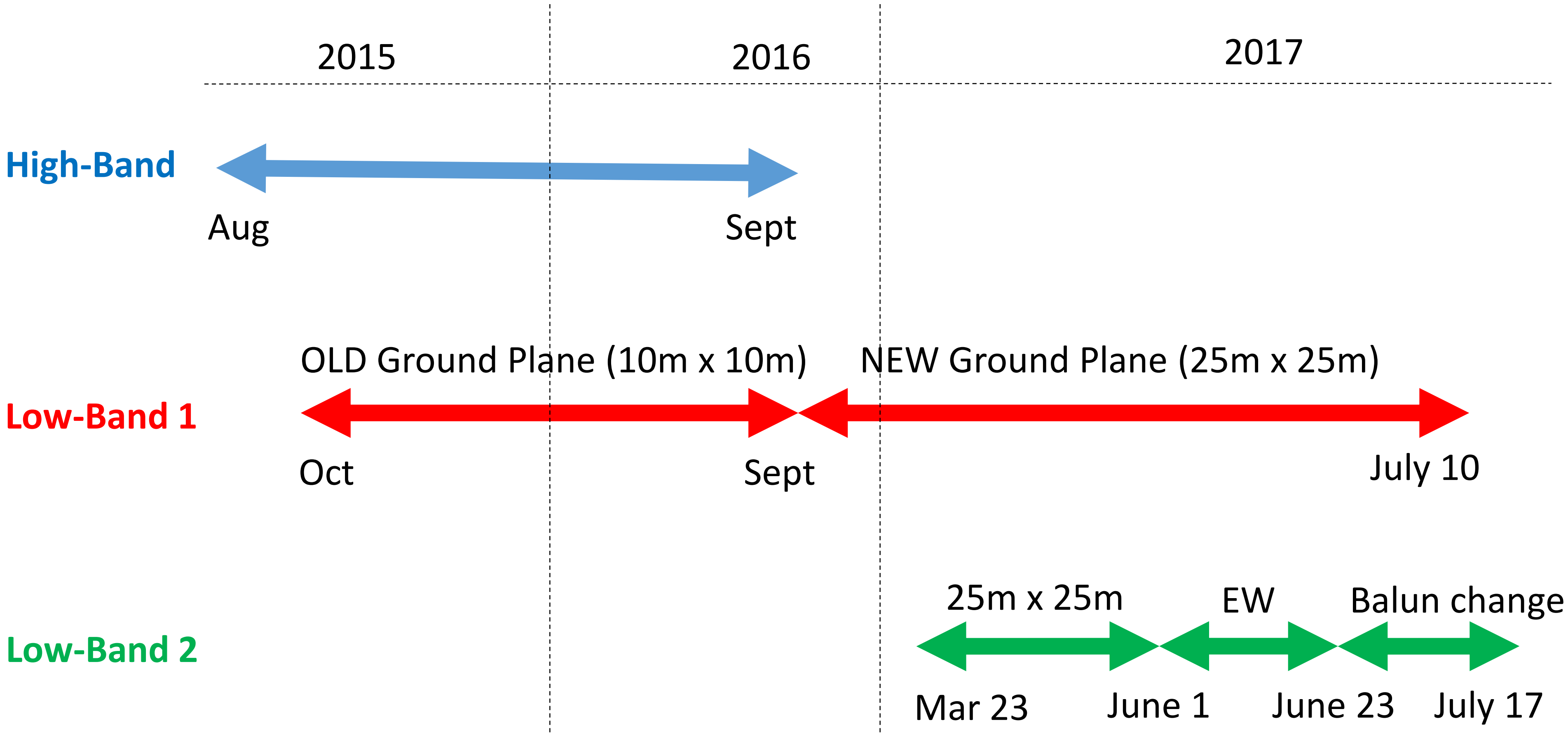

EDGES **High-Band** 2015-2016

Ground plane:
10m x 10m

Antenna size:
1m long / 0.5m high

EDGES **Low-Band 1** 2015-2016

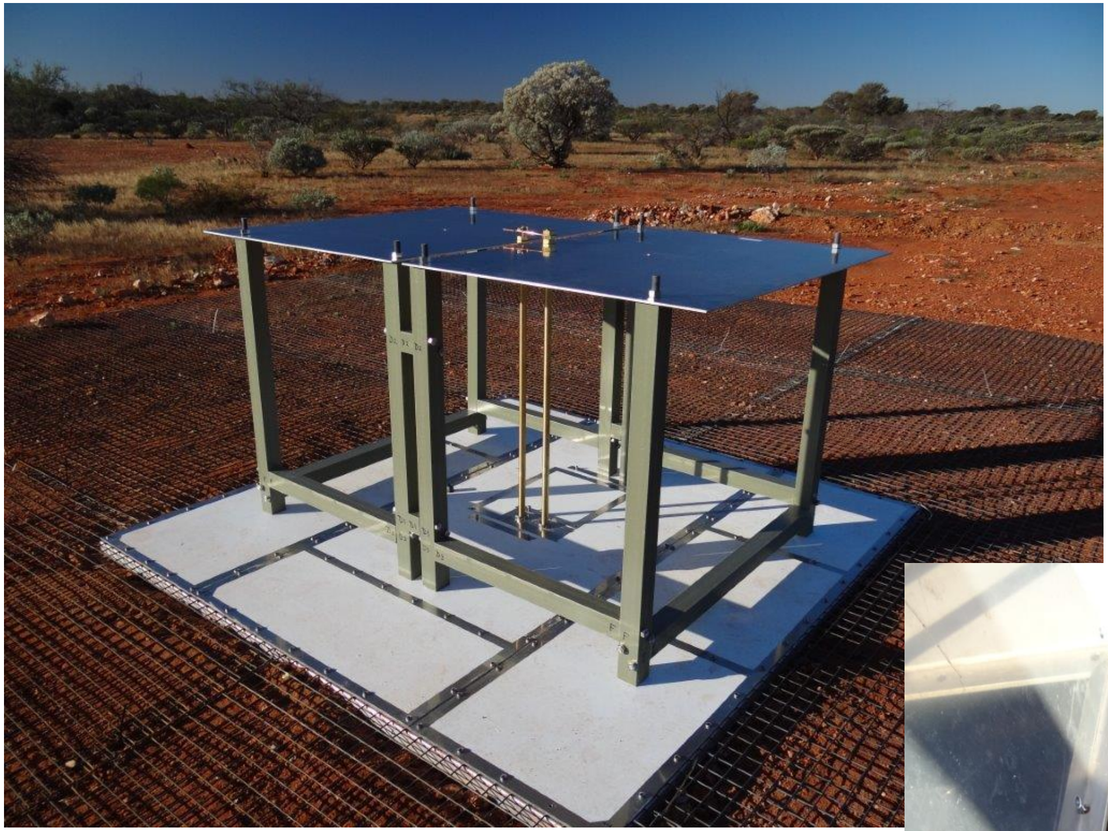

OLD Ground plane:
10m x 10m

Antenna size:
2m long / 1m high

Sept 2016 Low-Band 1 New Ground Plane

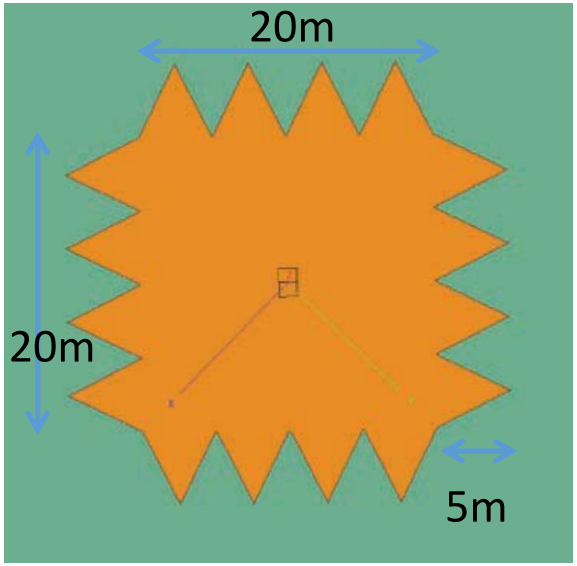

NEW Ground Plane:

Central Square: 20m x 20m

16 Triangles: 5m-long

OLD Ground Plane

NEW Ground Plane

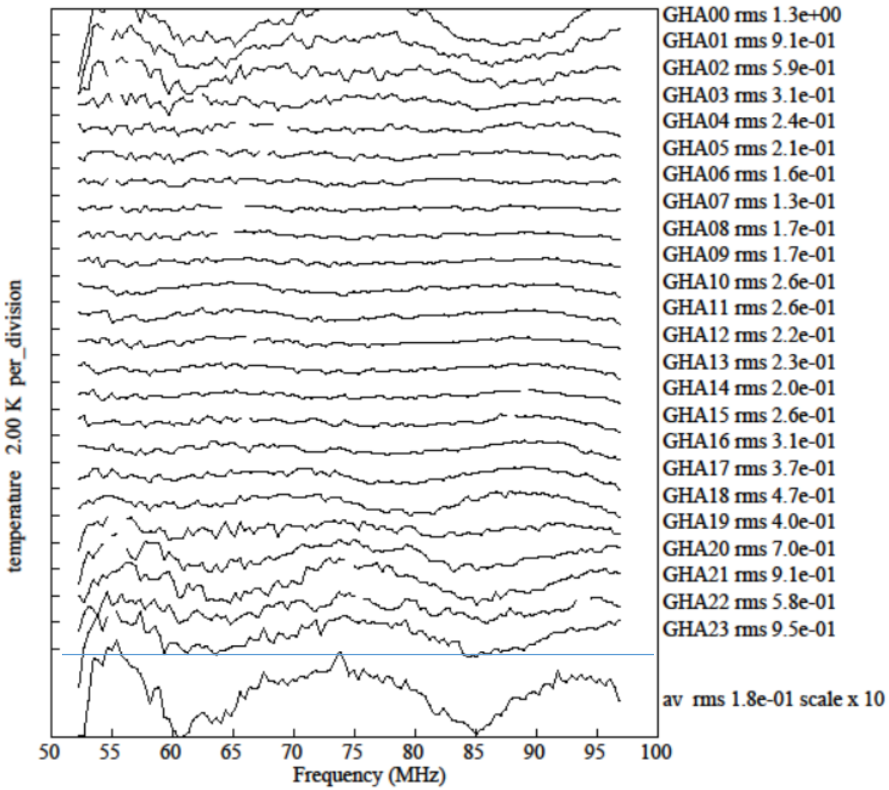

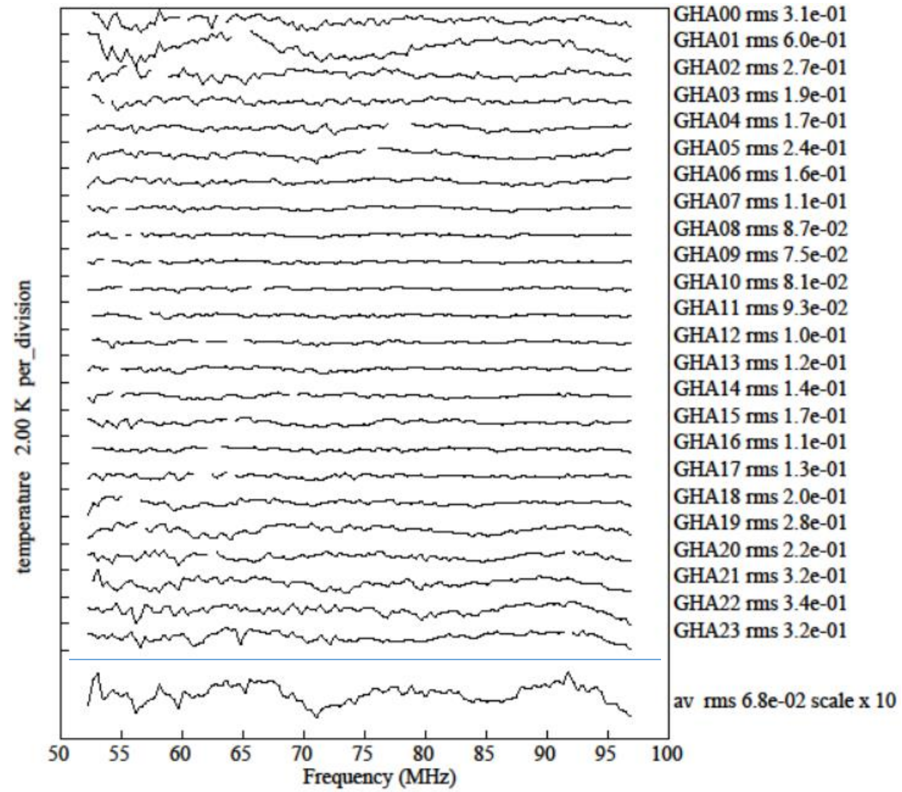

Example 10-day averages:

OLD

180 mK

NEW

68 mK

Factor ∼3 improvement due to NEW Ground Plane

March 2017 Low-Band 2 Instrument

EDGES 2017

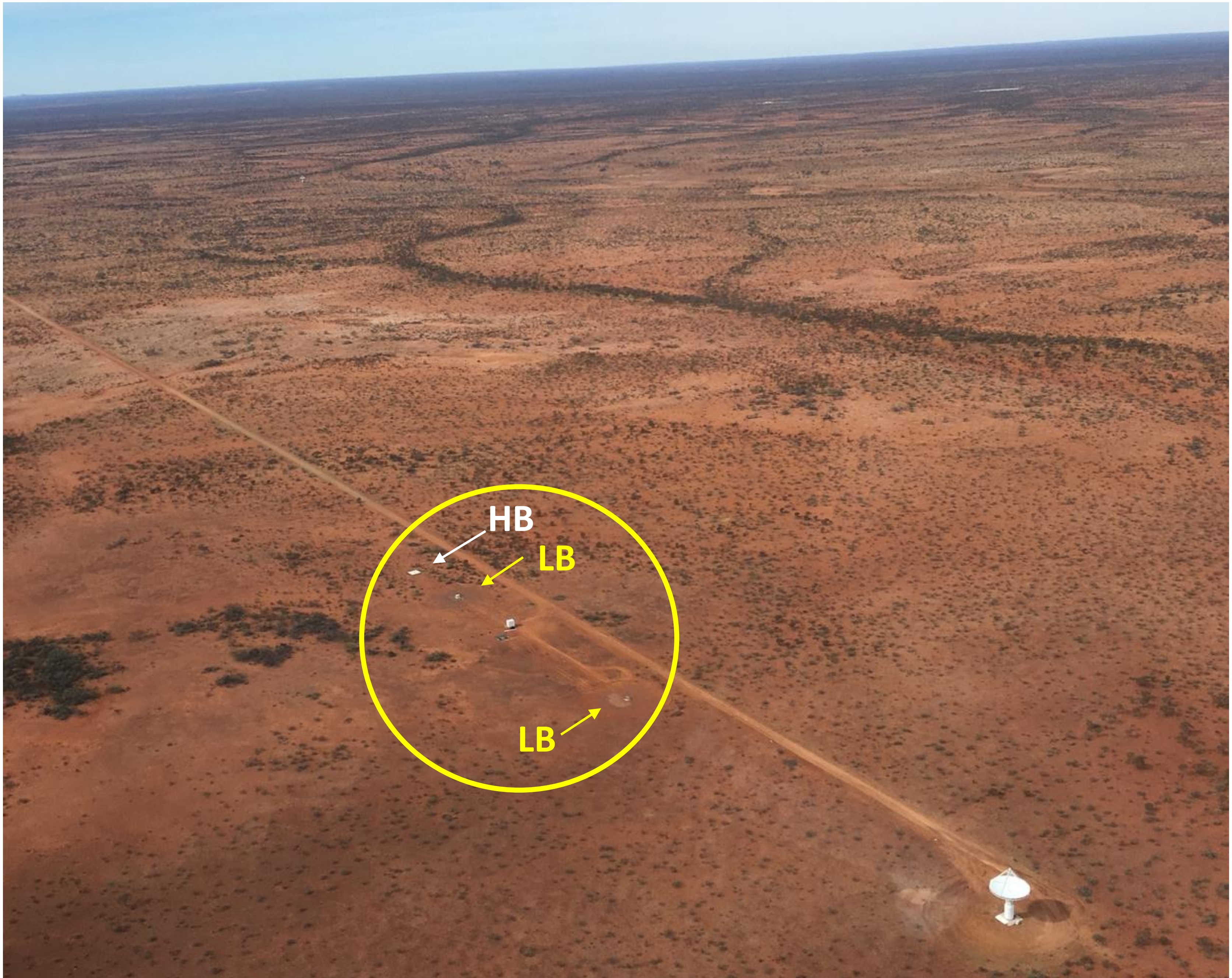

Instrumental Calibration

Calibration involves removing the following effects:

1) Receiver gain and offset.
2) Impedance mismatch between receiver and the antenna.
3) Antenna and ground losses.
4) Frequency-dependence of the antenna beam.

Observations

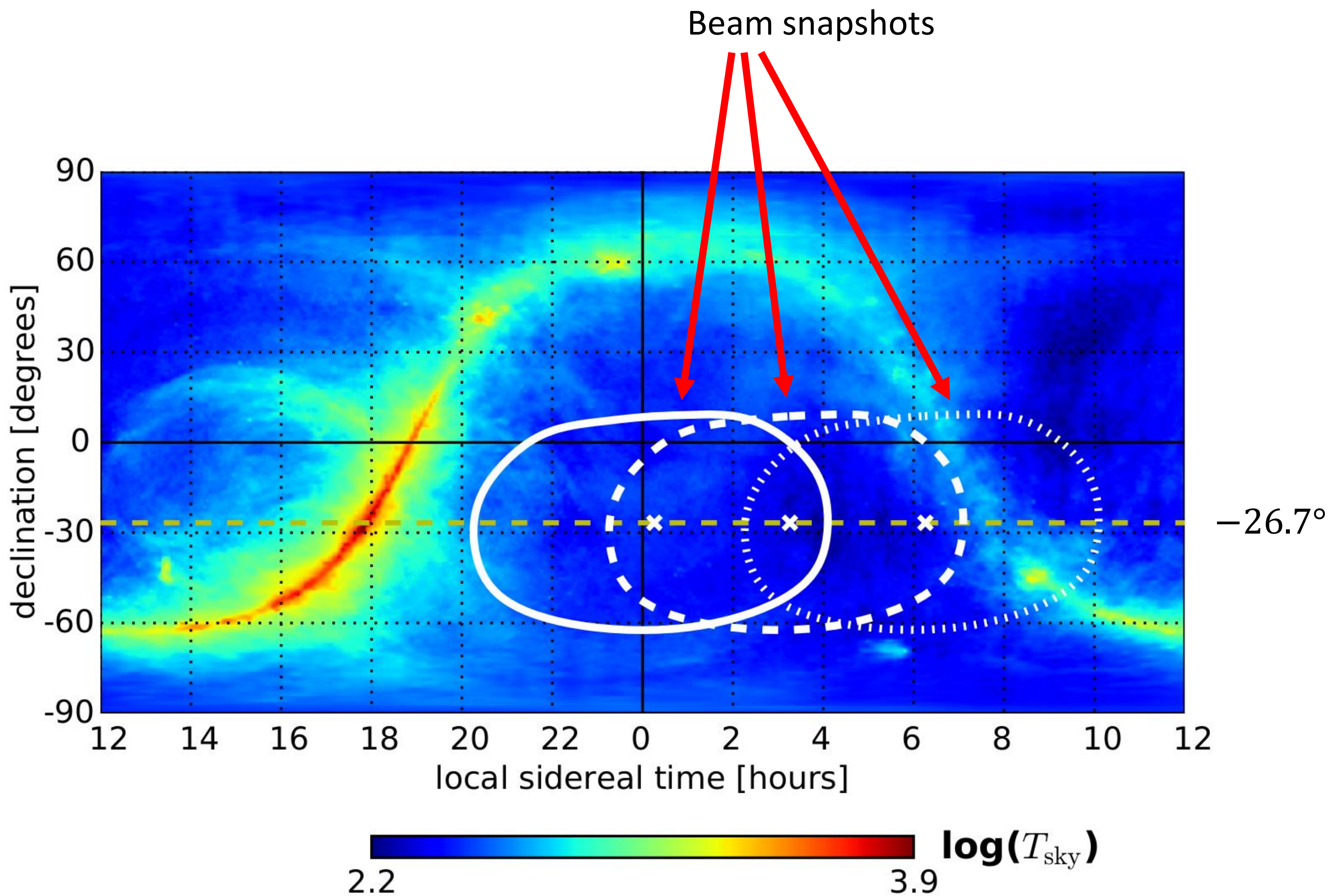

Observations

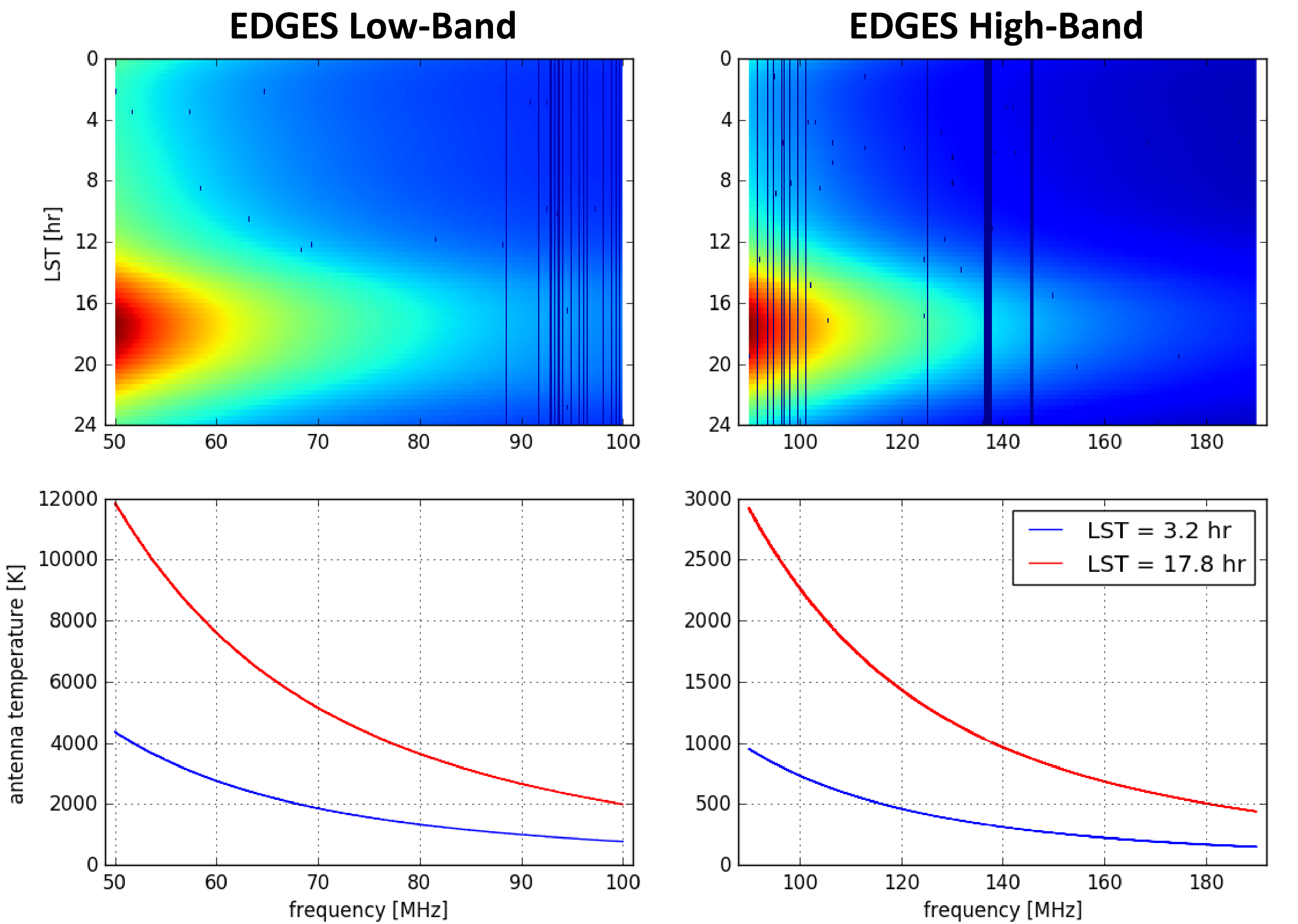

Beam chromaticity

Antenna-to-Sky Average Temperature

$$\langle T_{\mathrm{ant}}(\upsilon, \mathrm{LST}) \rangle_{\Omega} = \int T_{\mathrm{sky}}(\upsilon, \mathrm{LST}, \Omega) \cdot B(\upsilon, \mathrm{LST}, \Omega)\, d\Omega$$

$$\langle T_{\mathrm{ant}}(\upsilon, \mathrm{LST}) \rangle_{\Omega} = C(\upsilon, \mathrm{LST}) \cdot \langle T_{\mathrm{sky}}(\upsilon, \mathrm{LST}) \rangle_{\Omega}$$

Chromaticity Correction

$$C(\upsilon, \mathrm{LST}) = \frac{\int T_{\mathrm{sky}}(\boldsymbol{\upsilon_{\mathrm{ref}}}, \mathrm{LST}, \Omega) \cdot B(\boldsymbol{\upsilon}, \mathrm{LST}, \Omega)\, d\Omega}{\int T_{\mathrm{sky}}(\boldsymbol{\upsilon_{\mathrm{ref}}}, \mathrm{LST}, \Omega) \cdot B(\boldsymbol{\upsilon_{\mathrm{ref}}}, \mathrm{LST}, \Omega)\, d\Omega}$$

Simulated Antenna Beam at One Frequency

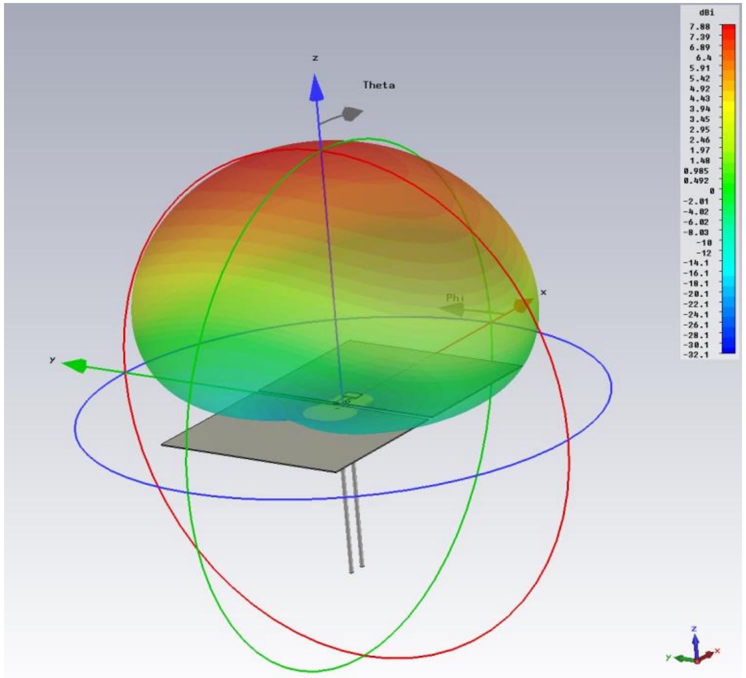

Chromaticity Correction

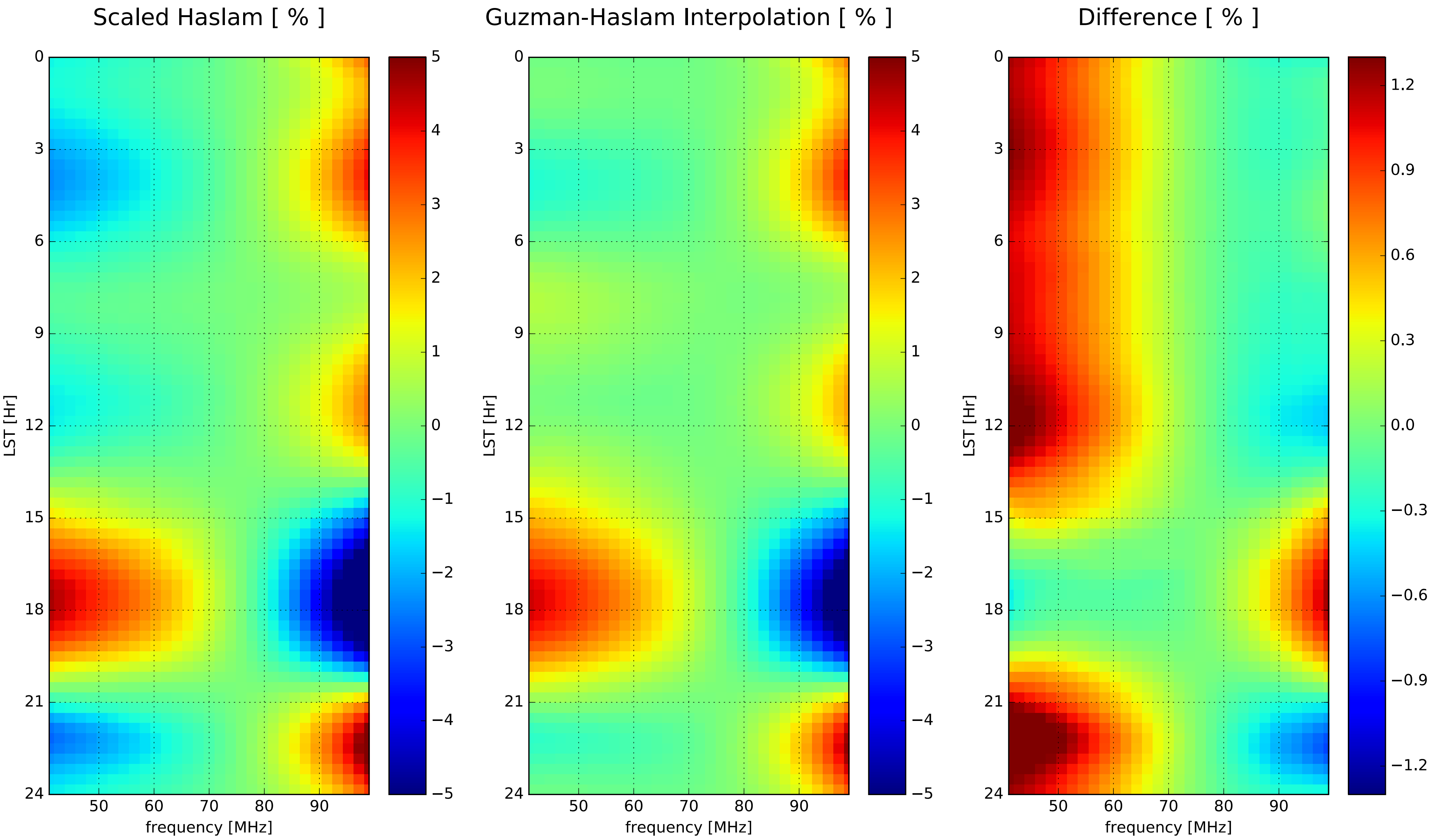

Beam-Weighted Spectral Index of Diffuse Foregrounds at DEC = −26.7°

Fit Model:
Two-parameter Power Law:

$$T_{\text{sky}}(\upsilon) = T_{150}\left(\frac{\upsilon}{150\ \text{MHz}}\right)^{+\beta} + T_{\text{CMB}}$$

Mozdzen et al. (2017)

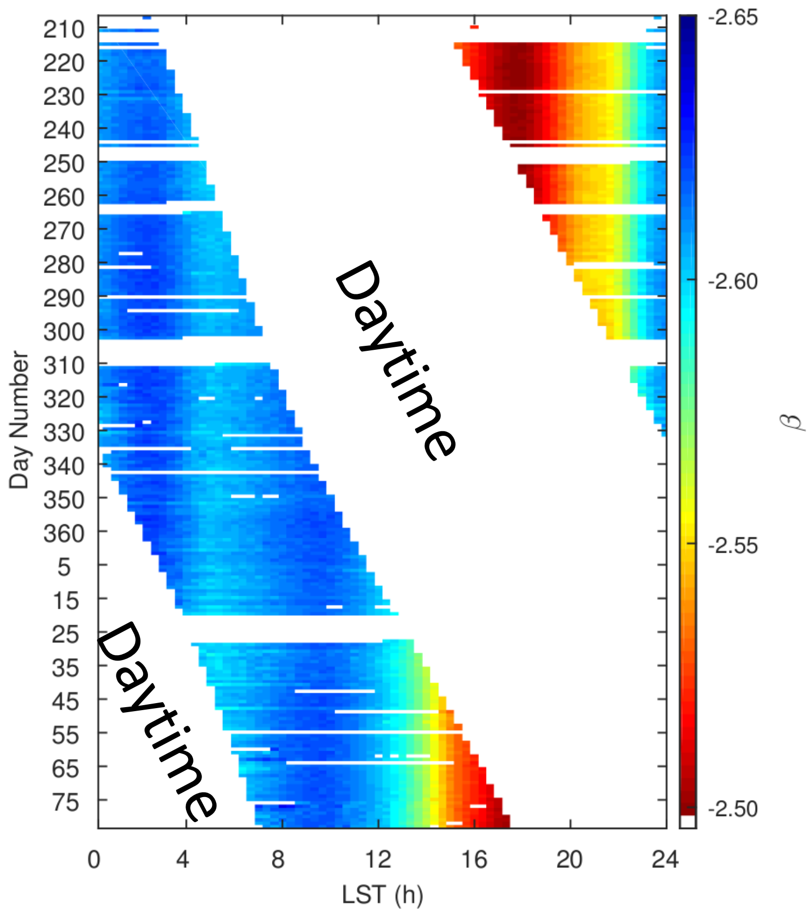

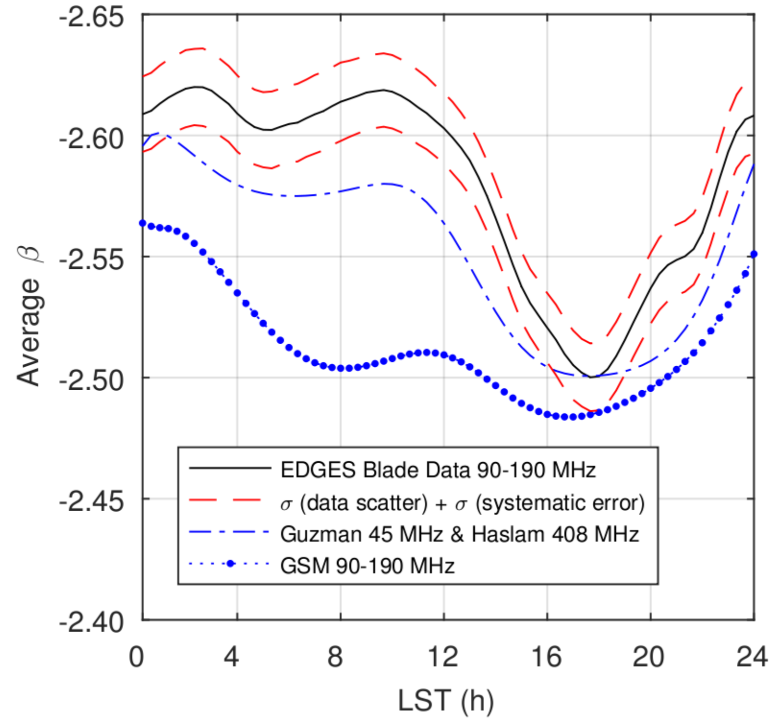

Previous result:
Rogers & Bowman (2008) estimated $\beta = -2.5 \pm 0.1$

Space-dependent Spectral Index

Example of discrepancies between the spectral index computed **from maps of the GSM-2008**, and directly **from the low-frequency measurements**.

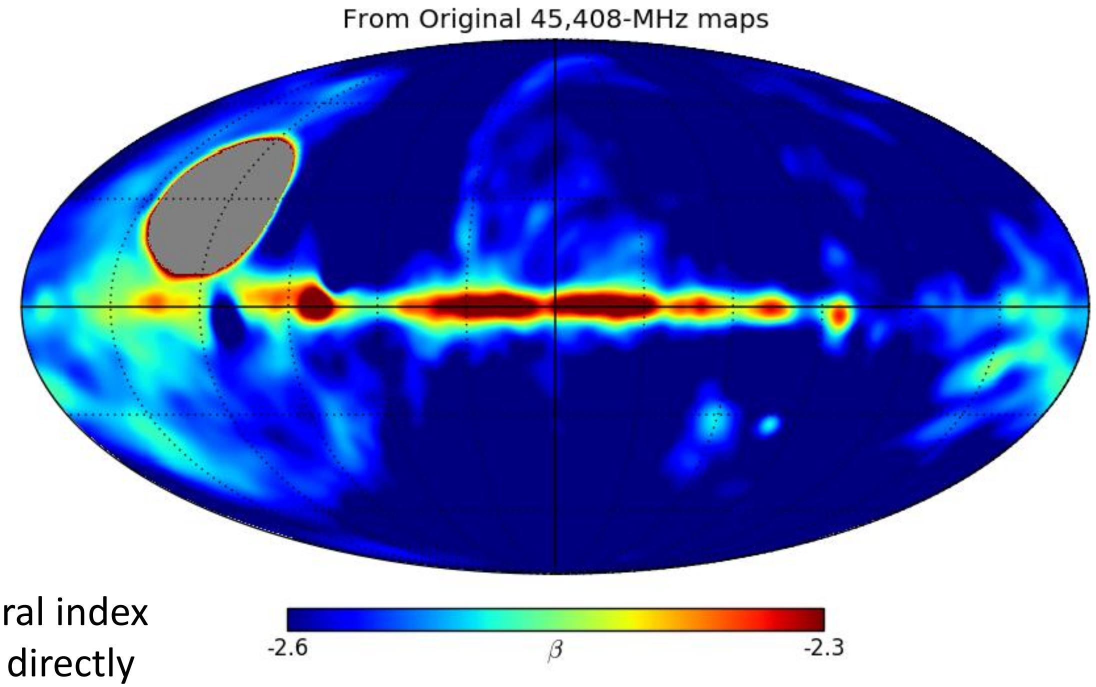

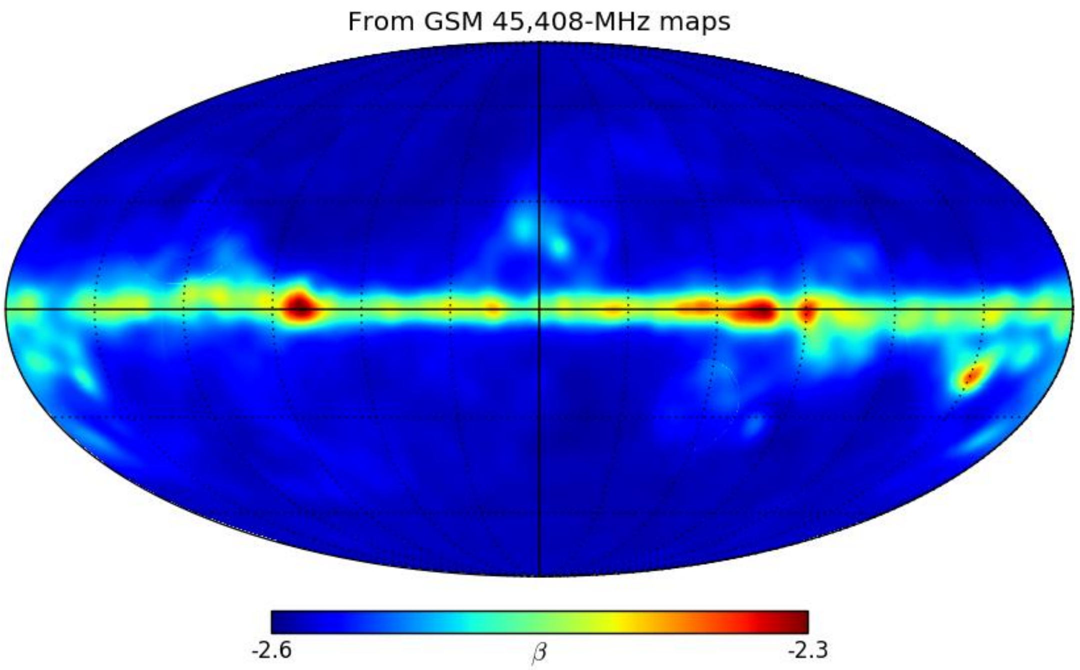

EDGES High-Band Observations from 2015

1. Residuals to 5-term polynomial
2. 40 days of nighttime
3. 6-hr averages
4. Low foregrounds
5. Typical daily RMS residuals ~ 60 mK

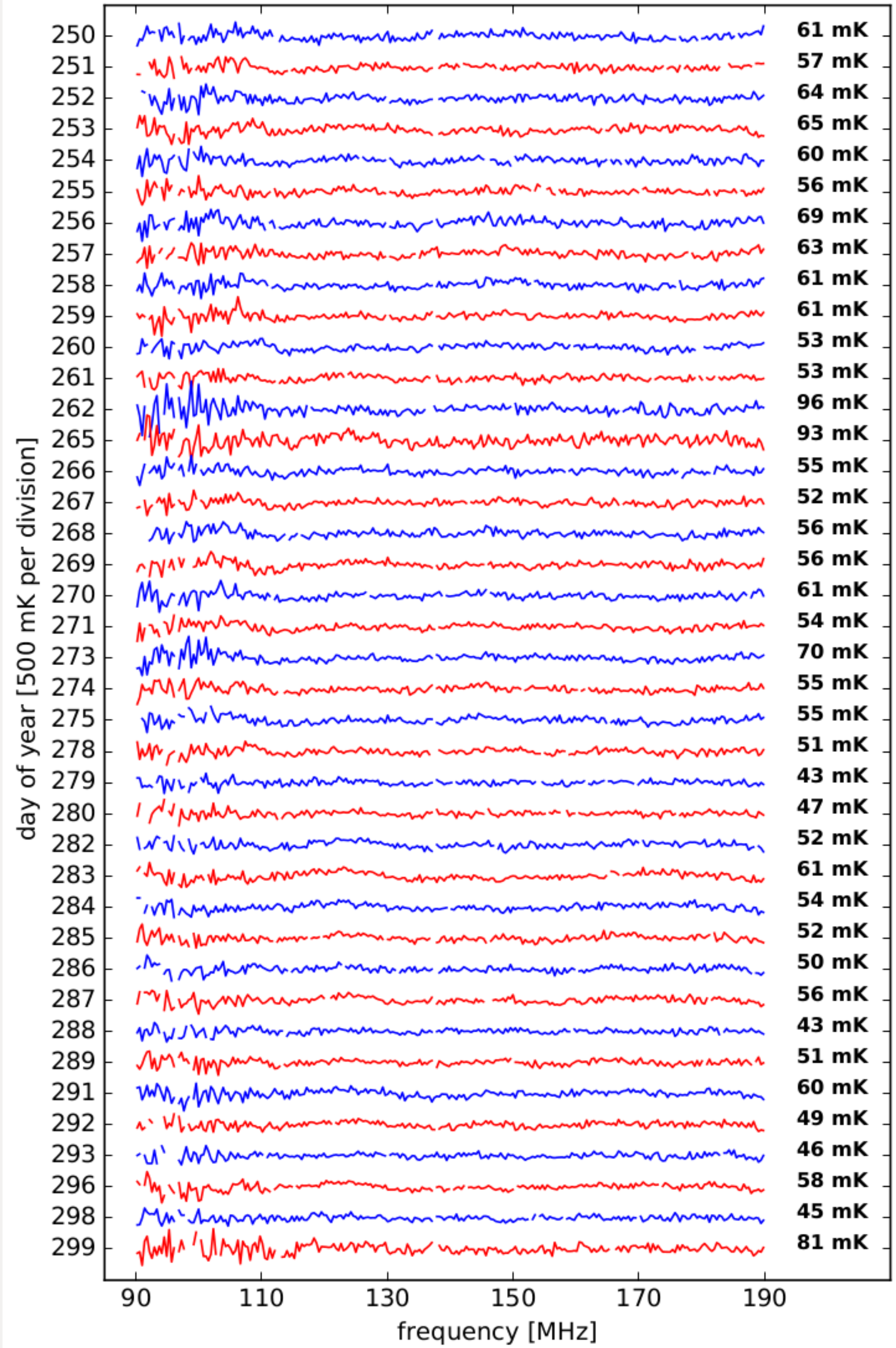

EDGES High-Band Observations from 2015

1. Residuals to 5-term polynomial
2. Average of 40 days of nighttime
3. 6-hr average
4. Low foregrounds

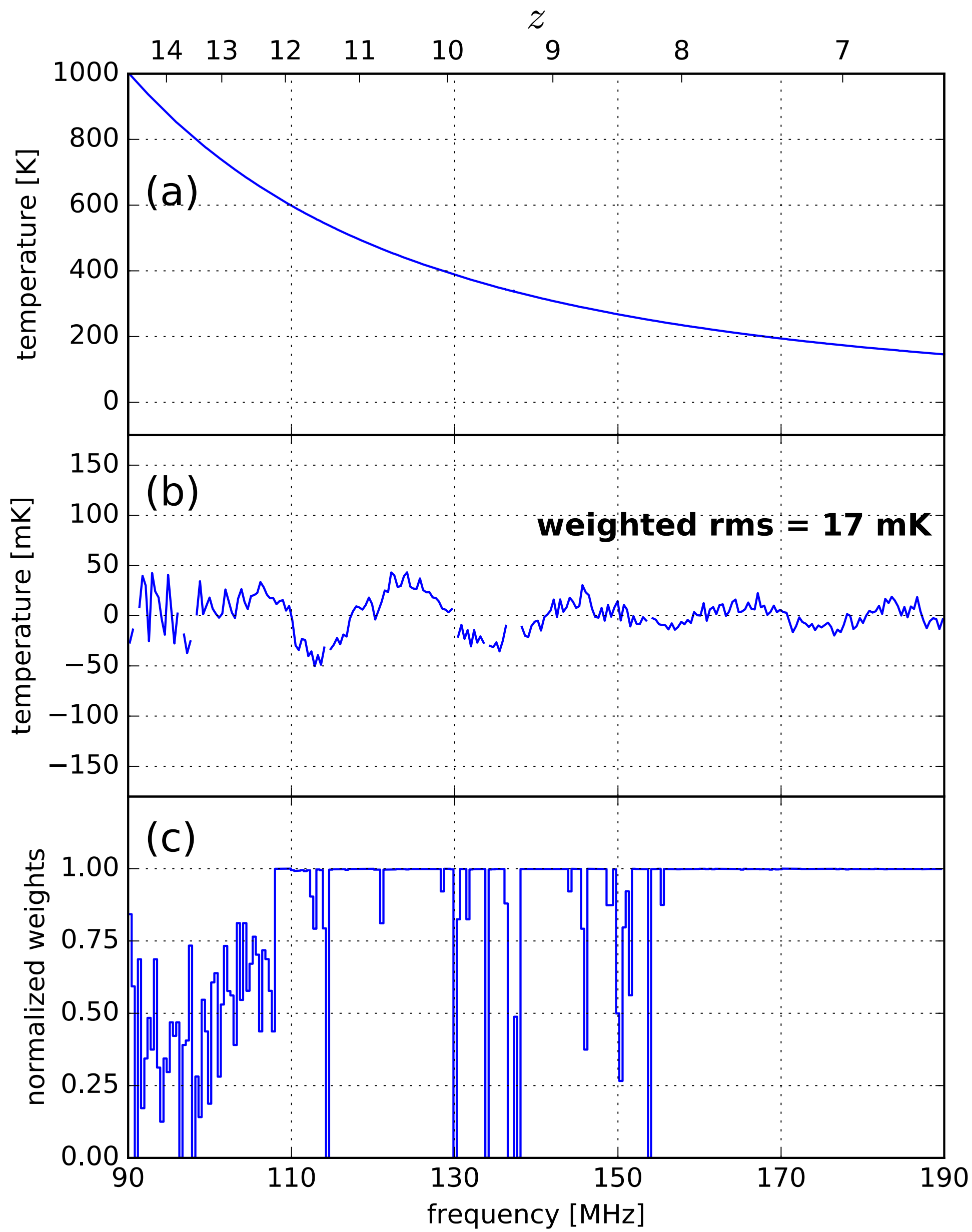

Parameter Estimation: Weighted Least Squares

Measurement model

$$d = T_{21} + T_{\mathrm{fg}} + \text{noise} \quad = \quad \boldsymbol{a_{21}}\,\mathrm{Model}_{21} + \left[\sum_{i=0}^{N_{\mathrm{fg}}-1} \boldsymbol{a_i}\,\upsilon^{-2.5+i}\right] + \text{noise}$$

Linear parameter vector

$$\lambda = [a_{21}, a_i]$$

Estimates

$$\hat{\lambda} = \left(A^T W A\right)^{-1} A^T W d \rightarrow \hat{a}_{21}$$

$$\hat{\Sigma} = \left(A^T W A\right)^{-1} \rightarrow \hat{\sigma}_{21}$$

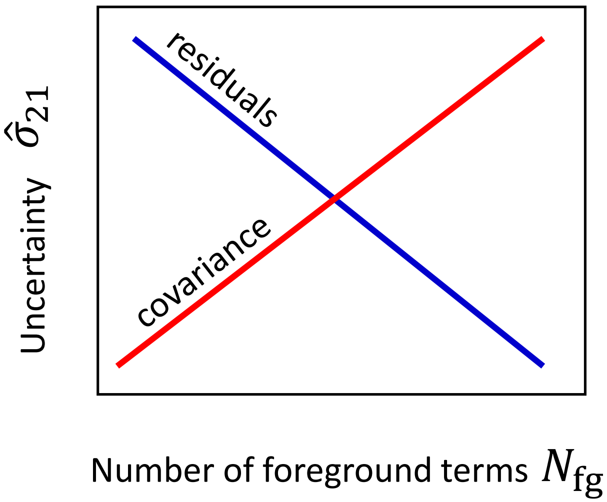

Rejection of Physical Models: Mirocha et al. (2017)

Galaxy Luminosity Function (LF): number density of galaxies per unit luminosity

Parameters explored:

1) Star formation rate density (SFRD).
2) Intrinsic UV and X-ray photon production of galaxies.
3) Escape of photons from galaxies.

Thousands of models available.

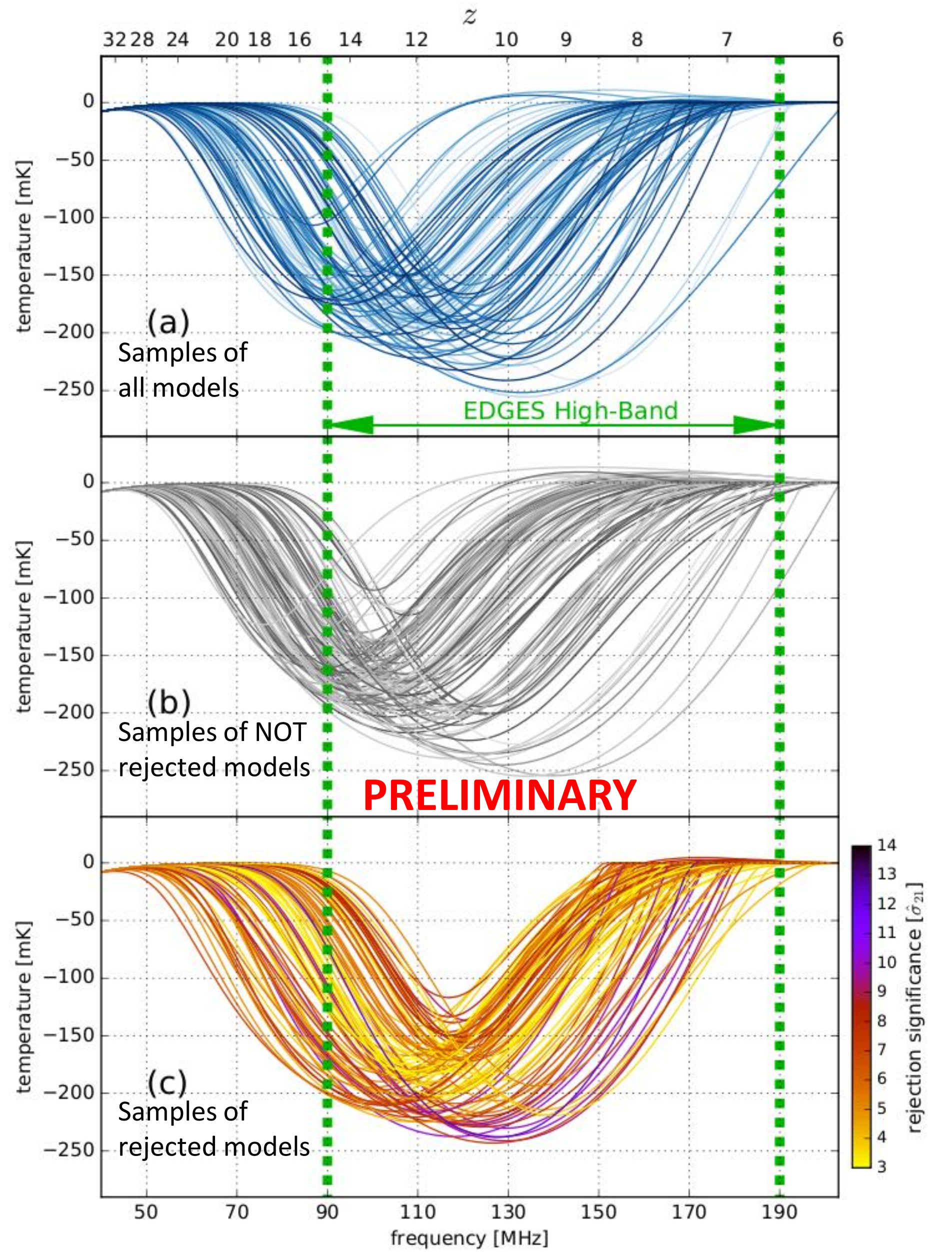

Monsalve et al., in preparation

Rejection of Physical Models: Mirocha et al.

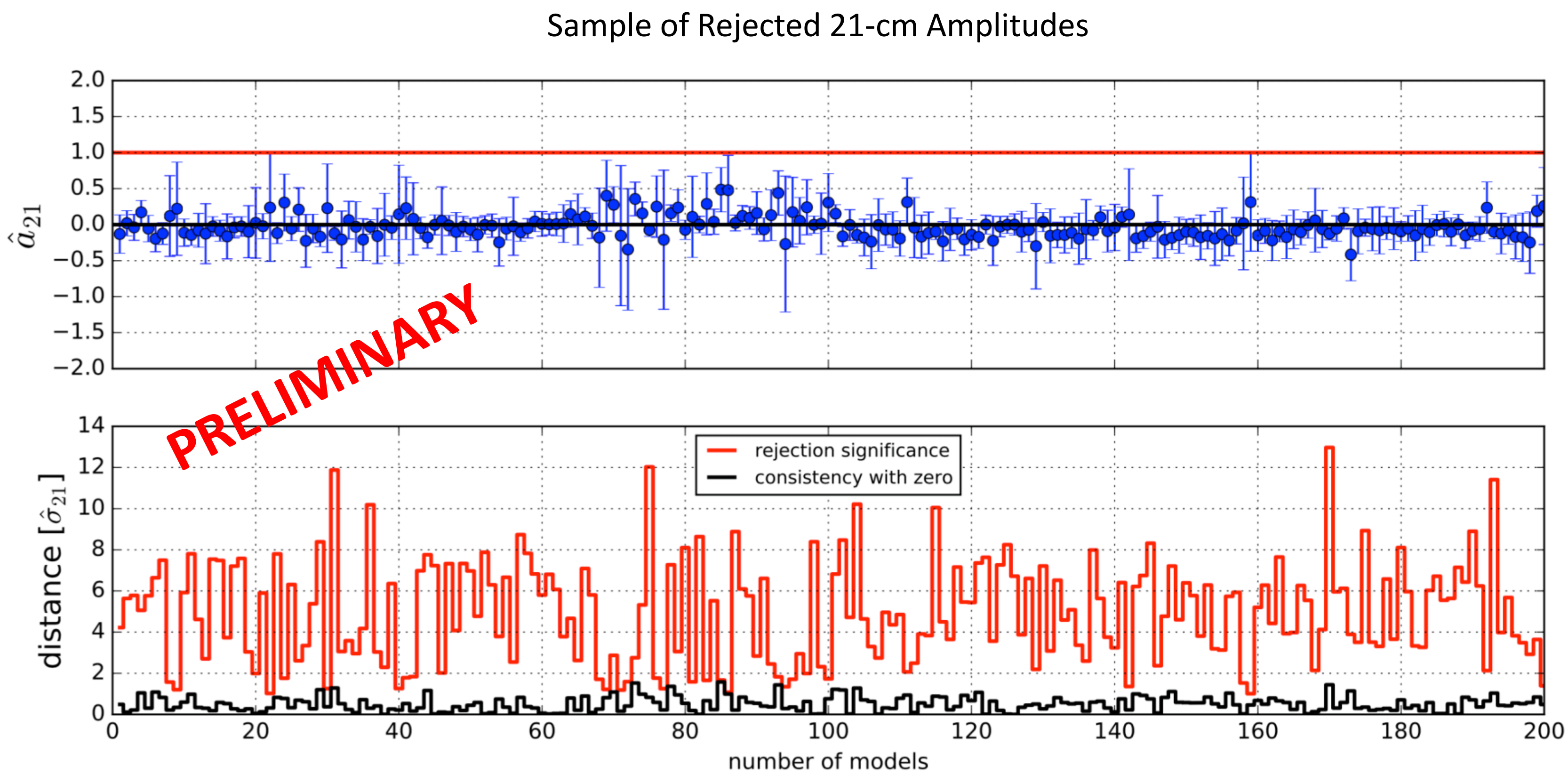

Monsalve et al., in preparation

Rejection of Physical Models: Fialkov, Cohen, Barkana.

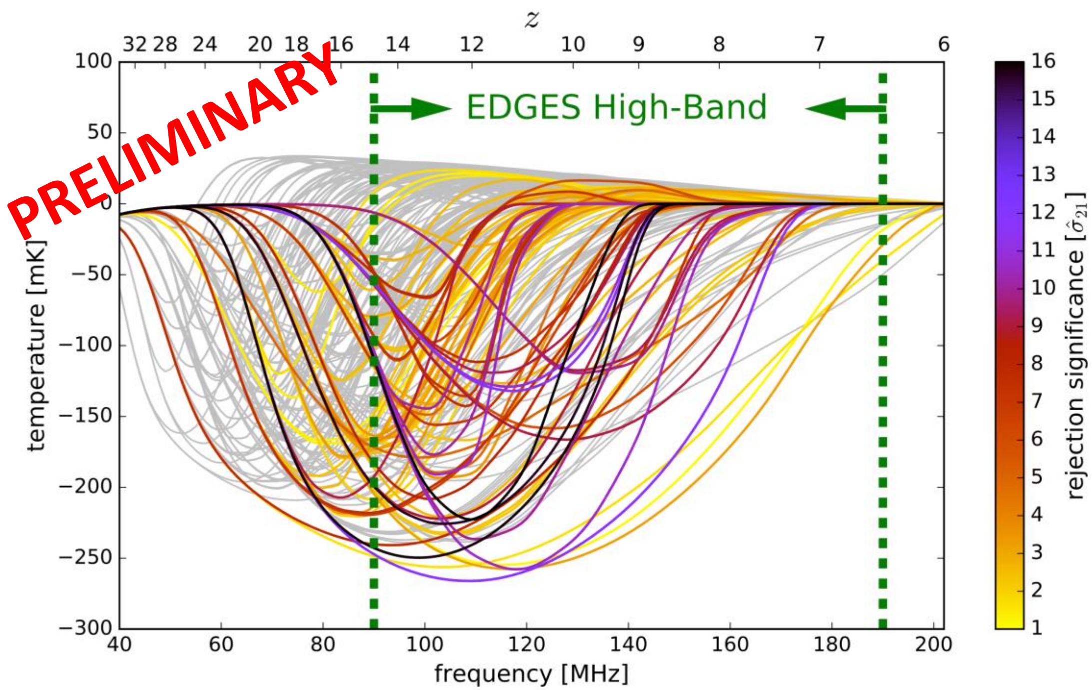

From numerical simulations:
Fialkov et al. (2016)
Cohen et al. (2017)

Parameters explored:

1) Star formation efficiency.
2) Minimal mass of star-forming halos.
3) Efficiency and spectral energy distribution of first X-ray sources.
4) History of reionization.

Monsalve et al., in preparation

Thousands of models available.

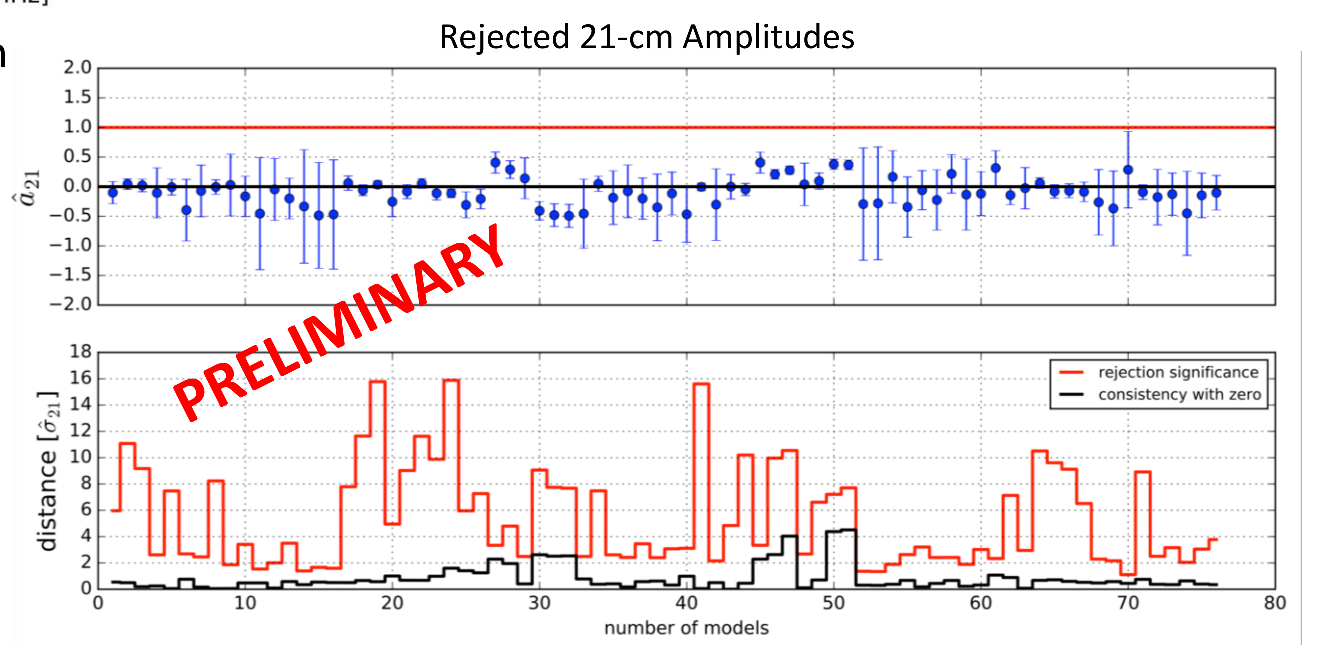

EDGES Low-Band 1: Sample of Observations (4-terms removed over 30-MHz Bandwidth)

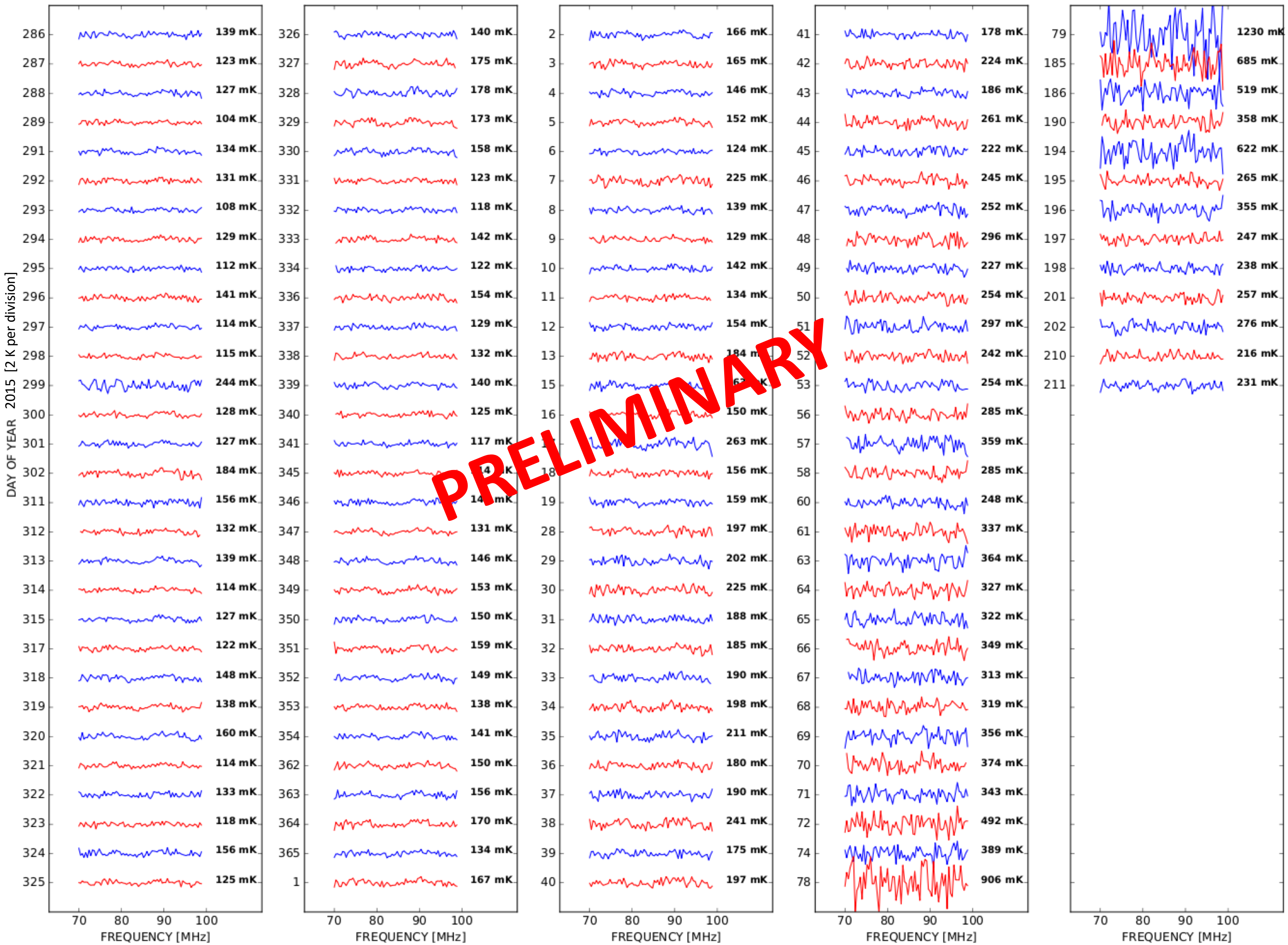

EDGES Low-Band 2: Sample of Observations (4-terms removed over 38-MHz Bandwidth)

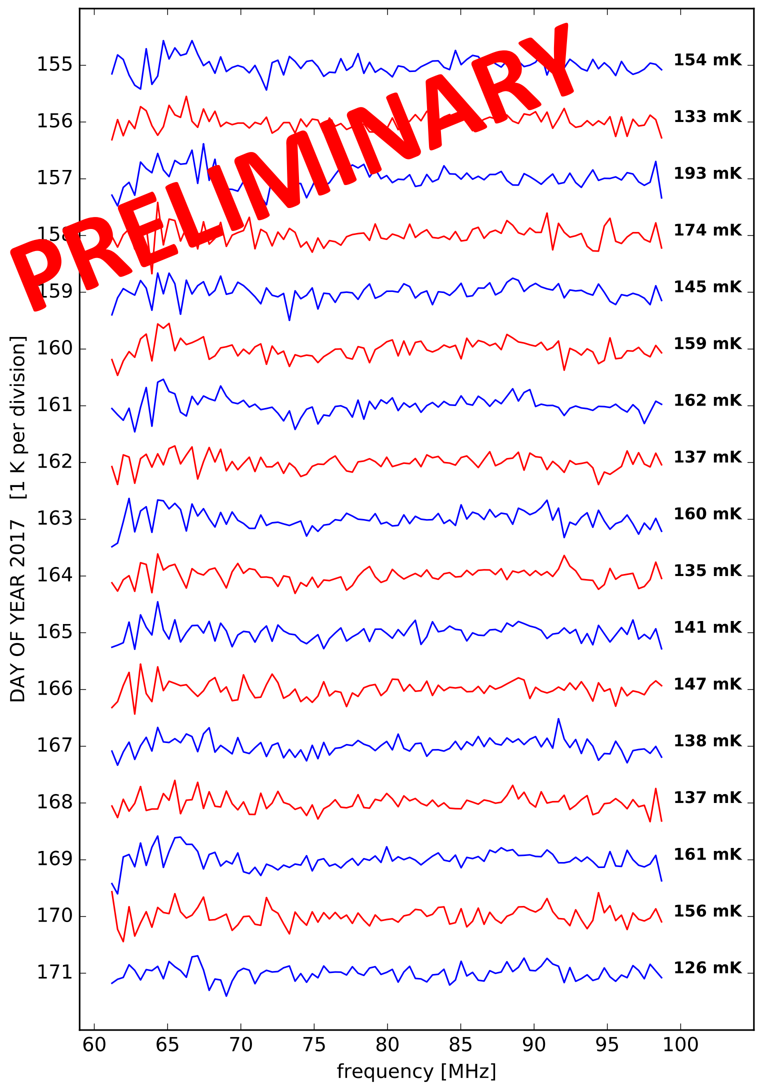

1) From **both Low-Band instruments** we have enough data to reduce the **noise below ~20 mK** over wide (>40 MHz) frequency ranges.

2) Carefully **exploring the consistency** of the different data sets, **using two independent processing pipelines**.

3) Main target is 21-cm signal, but enough data and sensitivity to conduct **refined spectral index study**. **Future Work.**

Diffuse Foregrounds Among Calibration Uncertainties

Uncertainties Assigned to Calibration Parameters

Parameter	1-σ Uncertainty
Receiver	
Temperature correction	0.1°C
Absolute calibration	from Monsalve et al. (2017) (*)
Antenna Reflection Coefficient	
Magnitude	10^{-4} in voltage ratio (*)
Phase	0.1° (*)
Antenna Losses	
Balun length	1 mm
Connector length	0.1 mm
Balun and connector radii	3%
Balun and connector conductivity	1%
Connector teflon permittivity	1%
Panel loss	10% (*)
Ground loss	10% of nominal + 30% from FEKO and CST (*)
Chromaticity Factor	
Foreground model	50% of difference between nominal and Zheng et al. (2017) (*)
Antenna panel height	2 mm
Antenna panel length	2 mm
Antenna panel width	2 mm
Antenna panel separation	1 mm
Ground plane length	5 cm
Ground plane width	5 cm
Antenna orientation angle	0.5°
Soil conductivity	50%
Soil relative permittivity	50%

Note. — (i) Unless otherwise noted, percentages are given as relative to the nominal value. (ii) The symbol (*) denotes frequency-dependent values.

Work in Progress

1) Implementing a rigorous **quantification and propagation** uncertainties.

2) Using **Singular Value Decomposition (SVD)** to find foreground and instrument orthogonal basis functions.

3) Incorporating all **diffuse foreground maps** available.

4) **Sampling** physical, instrumental, and foreground parameters **using MCMC**.

Summary

- **EDGES High-Band noise < 10 mK**.
- **Probing thousands of physical models,** produced analytically and numerically.
- **Ruling out large fractions of those** models with high significance.
- Estimated **B-W spectral index of diffuse foregrounds** with 0.01 uncertainty at DEC = $-26.7°$.
- **Low-Band noise < 20 mK**.
- Two Low-Band instruments, **in different configurations**, to distinguish the spectral features **intrinsic to the sky from those due to calibration systematics**.
- Intending to do a refined **Low-Band spectral index study** to complement High-Band results.

Thank you